Chapter 4
Median Subbetic Outcrops

4.1 Iznalloz Section

The Iznalloz (IZ) section is located in the km 13 of the Granada-Moreda railway scarpment (N 37° 23′ 24.4″; E 03° 29′ 19.5″), 3 km east of the village of Iznalloz (Granada Province, Figs. 3.1 and 4.1). The study section pertains to the Toarcian of the Zegrí Formation, and contains alternating marls and marly limestones in the lower part with nodular marly limestones (ammonitico rosso facies) in the upper part (Braga et al. 1981; Reolid et al. 2015).

The studied interval in the Iznalloz section is 18.5 m-thick. It comprises 3.2 m of yellow limestones, marls and marly limestones (Polymorphum and Serpentinum zones), 6.8 m of red marls and marly limestones having a nodular appearance, with intercalations of white laminated limestones (Bifrons and lower part of Gradata zones), and 8.5 m of nodular limestones and marly limestones (from upper part of Gradata Zone to Aalensis Zone) (Figs. 4.1 and 4.2).

The Iznalloz section was initially studied by Mouterde and Linares (1960), Rivas (1972), Braga et al. (1981) and Jiménez (1986), with special emphasis on the ammonite biostratigraphy, whereas Palomo (1987) focused on clay minerals. Recently, Reolid et al. (2015) studied the lithofacies and trace fossils. In this section the T-OAE is not well represented due to the thickness of the Polymorphum and Serpentinum zones, the presence of stratigraphic gaps as well as the environmental conditions of this setting favouring the oxygenation. However, this section presents a very different set of lithofacies during the Toarcian that help in the understanding of the evolution of the South Iberian Palaeomargin.

4.1.1 Ammonite Biostratigraphy

The Iznalloz section is very rich in ammonites and belemnites, favouring a fine biostratigraphy both in the marly interval and in the red nodular limestones (Rivas

M. Reolid et al., *The Toarcian Oceanic Anoxic Event in the South Iberian Palaeomargin*, SpringerBriefs in Earth Sciences,
DOI 10.1007/978-3-319-67211-3_4

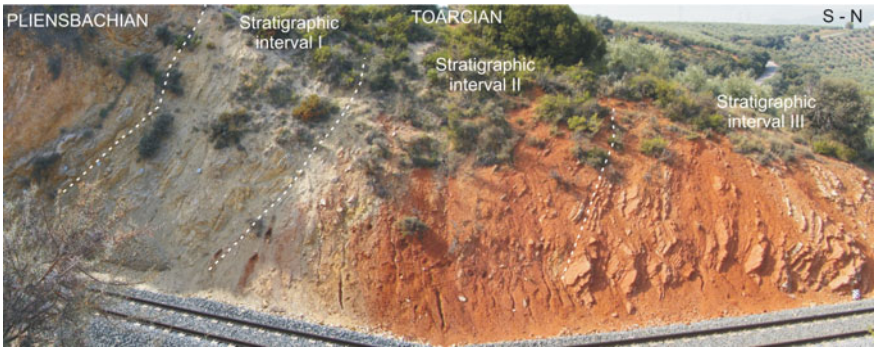

Fig. 4.1 Field view of Iznalloz section and differentiates stratigraphic intervals for the Toarcian. Note the inverted disposition of the stratigraphic succession

1972; Jiménez 1986). Above the micritic limestones of the upper Pliensbachian, three stratigraphic intervals have been differentiated in the Toarcian of the Iznalloz section (Reolid et al. 2015; Figs. 4.1 and 4.2).

- First stratigraphic interval (3.2 m): is formed by grey to yellow limestones, marls and marly limestones with *Dactylioceras polymorphum*, *D. simplex*, *Hildaites serpentinus* and *Murleyiceras evagriori*, among others (Rivas 1972; Jiménez 1986). This assemblage characterises the Polymorphum and Serpentinum zones (Lower Toarcian).
- Second stratigraphic interval (6.1 m): is composed of grey and red marls and marly limestones with a nodular appearance, featuring intercalations of white laminated limestone beds at a decimetric scale. In this interval, the ammonites *Catacoeloceras* sp., *Hildoceras bifrons*, *H. sublevisoni*, *H. semipolitum*, *Mercaticeras mercati* and *Nodicoeloceras* sp., determine the Bifrons Zone (Rivas 1972; Jiménez 1986). The record of *Brodieia gradata* and *B. bayani* at the top of this stratigraphic interval indicates the base of the Gradata Zone (middle Toarcian).
- Third stratigraphic interval (8.5 m-thick): is constituted by nodular limestones and secondarily nodular marly limestones, marls and white laminated limestones. The record of *Brodieia gradata*, *Chartronia elegans*, *Ch. iserensis* and *Phymatoceras* sp. indicates the Gradata Zone (Middle Toarcian) at the beginning of this stratigraphic interval. The presence of *Pseudogrammoceras fallaciosum* indicates the beginning of the Upper Toarcian (Fallaciosum Zone) from the base of bed IZ-18. The record of *Dumortieria latiumbilicata* and *Catulloceras meneghinii* characterise the Reynesi Zone, and the occurrence of *Erycites* sp., *Pleydellia subcompta* and *P. aalensis* from upper part of the IZ-23 confirms the beginning of the Aalensis Zone.

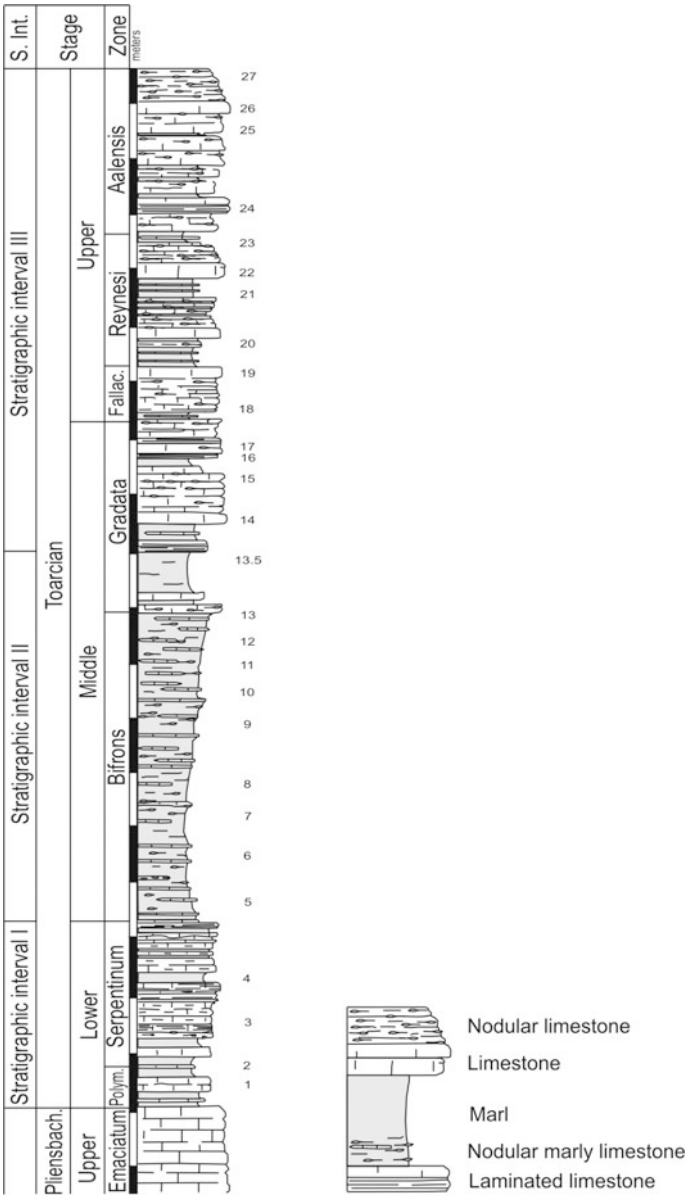

Fig. 4.2 Lithological column of the Iznalloz section. Biostratigraphic intervals according to Rivas (1972) and Jiménez (1986)

4.1.2 *Lithofacies and Microfacies*

Four main types of lithofacies were differentiated according to macroscopic and microscopic features (Figs. 4.2, 4.3, 4.4 and 4.5):

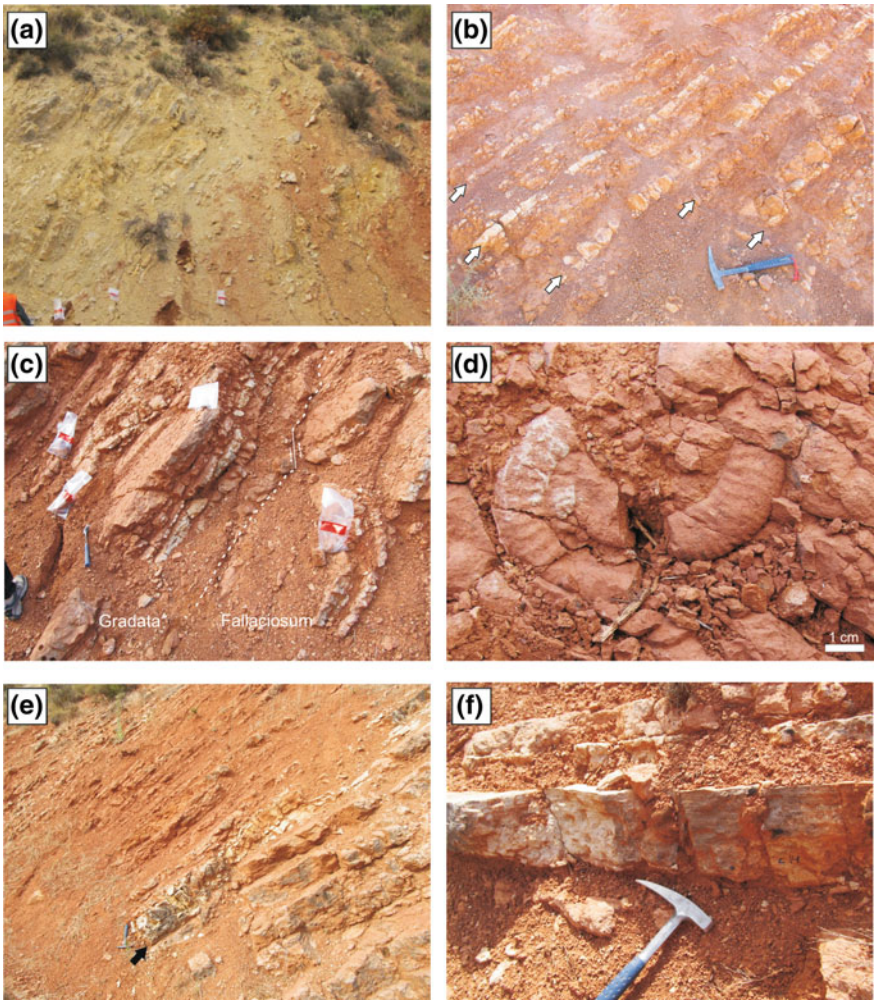

Fig. 4.3 Field view of lithofacies. **a** Grey-yellow limestones (Lower Toarcian, *left*) and grey marls (lower part of Bifrons Zone, Middle Toarcian, *right*). **b** Red marls from upper part of Bifrons Zone (Middle Toarcian) with thin white laminated limestones (*white arrows*). **c** Red nodular limestone (ammonitico rosso facies) from the boundary between Gradata Zone (Middle Toarcian) and Fallaciosum Zone (Upper Toarcian). **d** *Ericites* sp. close to Reynesi-Aalensis zone boundary. **e** *White* laminated limestone (*white arrow*) intercalated in ammonitico rosso facies of red nodular limestones from the base of Aalensis Zone (Upper Toarcian). **f** White laminated limestone from the upper part of Gradata Zone

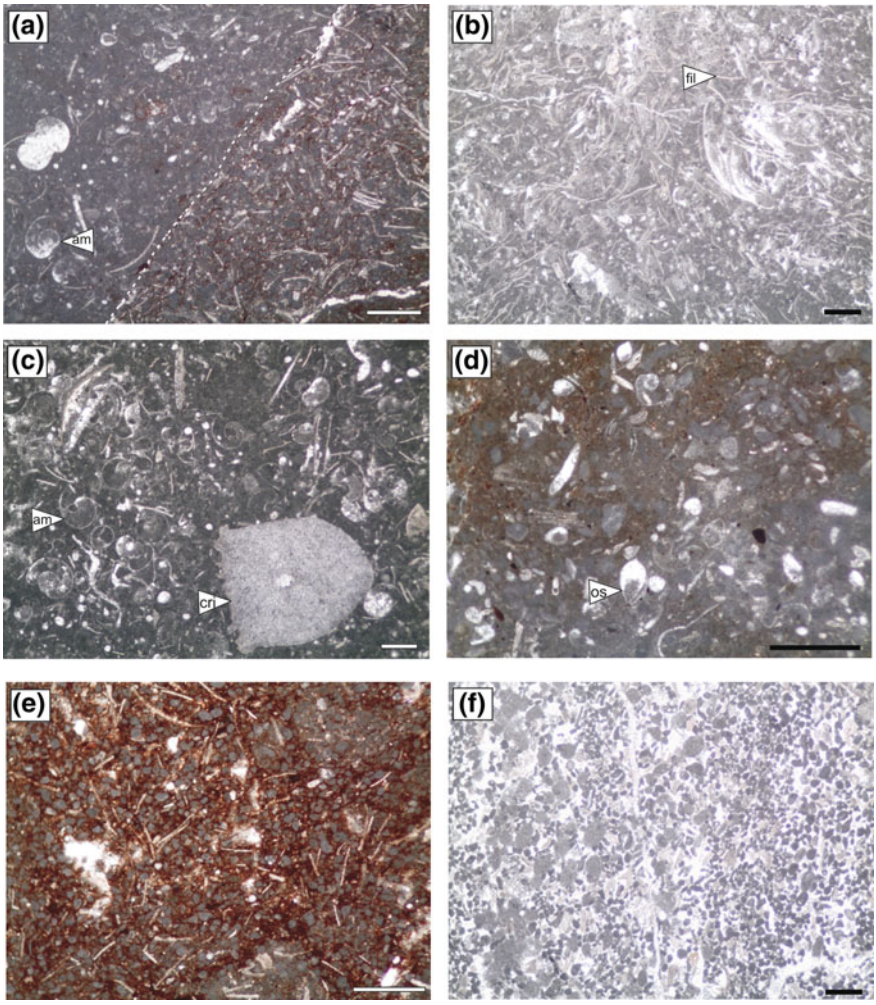

Fig. 4.4 Microfacies from Iznalloz section. **a** Contact between calcareous nodule (*left side*) rich in ammonitella and ostracods, and red clay rich matrix (*right side*) rich in fragments of filaments and iron oxides, indicated by a *dotted line* (Aalensis Zone). **b** Packstone of peloids and filaments from red nodular limestone (base of Gradata Zone). **c** Packstone of ammonitellas and echinoderm fragments from nodules (Aalensis Zone). **d** Packstone of bioclasts rich in ostracods and foraminifera from red pseudonodular marly limestone bed (Bifrons Zone). **e** Packstone of peloids and filaments from the clay rich matrix between nodules of the red nodular limestones (Reynesi Zone). **f** Laminated grainstone of peloids from white laminated limestone (Bifrons Zone). *Note* fil, filaments; am, ammonitella; cri, crinoid ossicle; os, ostracod. Scale bar 1 mm

(a) Grey-yellow limestones (Fig. 4.3a): Mudstone-wackestone of bioclasts at the base of the section, and packstone of peloids and filaments (thin shelled bivalves in larval stages with planktotrophic lifestyle). The grain size is very

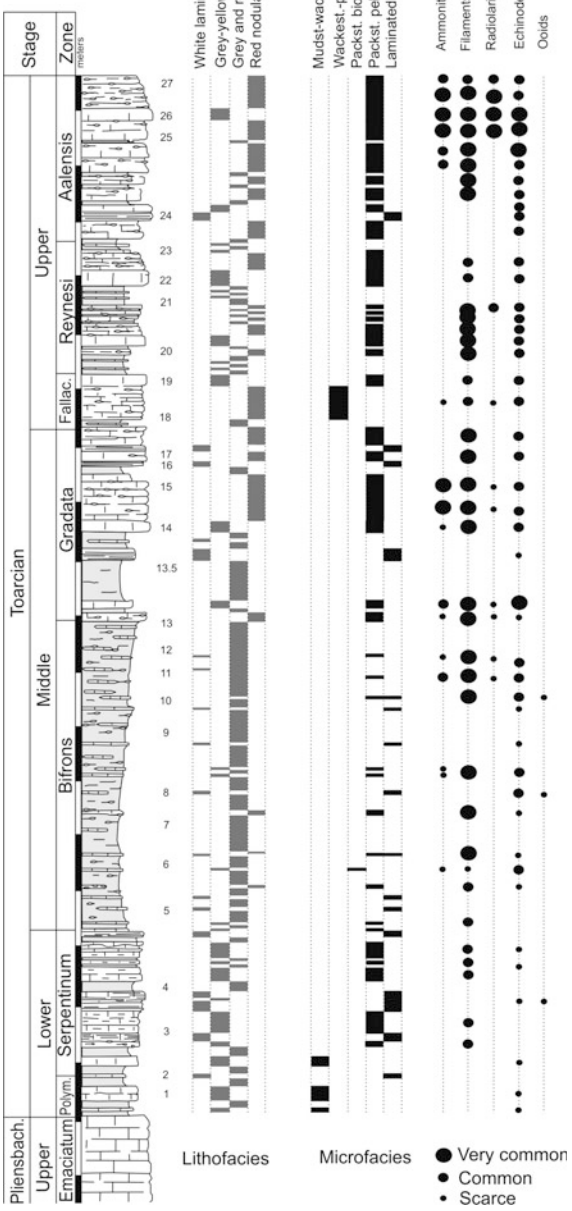

Fig. 4.5 Lithological column and stratigraphic distribution of lithofacies, microfacies and selected components of microfacies

fine (<100 μm). The most abundant bioclasts are filaments and echinoderms. Trace fossils are scarce and undifferentiated. This lithofacies constitutes the first stratigraphic interval (Lower Toarcian, Fig. 4.5). Marly layers between limestones contain illite, smectite and chlorite, but no kaolinite (Palomo 1987).

(b) Grey and red marls (Fig. 4.3b): They constitute most of the second stratigraphic interval (Middle Toarcian *p.p.*), with a predominance of grey marls in the lower part and red marls in the upper part. They present common microfossils such as foraminifera, ostracods and ophiuroids. Palomo (1987) indicated illite as the main component of clay minerals, with higher contents of smectites in the grey marls and higher contents of kaolinite in the red marls.

(c) Red nodular limestones and marly limestones (Fig. 4.3c–e): These are red beds 10–45 cm-thick and pseudonodular to nodular appearance, with a continuous subfacies transition from limestones (calcareous ammonitico rosso) to marly limestones (marly ammonitico rosso). This lithofacies is dominant in the third stratigraphic interval. The base of these beds is commonly rich in subhorizontal trace fossils. These limestones correspond mainly to packstone of peloids and filaments, a minority being wackestone-packstones of bioclasts (Fig. 4.4a–e). The matrix among grains is reddish and iron-rich, while peloids and lumps are grey. Filaments and echinoderms are the most common bioclasts. Filaments are usually not-oriented or oriented according to nodule edges. Reolid et al. (2015) indicate that the reddish matrix shows fluidal appearance in some samples. In Gradata and Aalensis zones, ammonitella (embryonic shells of ammonoids) are common; while radiolarians are common mainly at the top of the Aalensis Zone. This lithofacies appears in the Bifrons Zone as decimentric beds among marly beds (marly ammonitico rosso), and is predominant in the upper part of the Gradata Zone, where there is an increase in carbonate content, thickness and nodularity (calcareous ammonitico rosso). In the beds of the Bifrons Zone and in the Gradata Zone to base of the Aalensis Zone, the nodules are diffuse, showing very irregular shape and lighter colour with respect to the red background. In Reynesi and Aalensis zones, the white-grey nodules (1.5–3.5 cm) are clearly differentiated from the red internodule matrix in short sequences of increasing nodularity in each bed. In some cases, the nodulous aspect is restricted to the top of the beds. They are irregular nodules distributed in the beds as nodule-rich horizons (floated), and the contact between nodules and internodules is well-marked by the colour. The topmost metre of the section presents large nodules (1.5–5 cm) with spheroidal shape, the sharp edges sometimes in contact (not floating in the internodule matrix) with stylolites. Examination at thin section of this lithofacies shows a compact packing of peloids (with microstylolites) resulting in a packstone of filaments and peloids and a fluidal texture in the internodule; in turn, the nodules are packstone-wackestones of peloids with high amounts of ammonitella, filaments and radiolarians. Clay analyses of marly interlayers and nodular marly limestones by Palomo (1987) indicate a dominance of illite, high contents in kaolinite and the absence of smectites.

(d) White laminated limestones (Fig. 4.4e, f): This lithofacies is externally laminated and characterised by abundant trace fossils at the base. They are isolated beds 5–35 cm-thick (usually less than 15 cm), within the other lithofacies. They present parallel lamination that is well developed at the base of the bed, where fragmented remains of ammonites, brachiopods and bivalves are also recorded. Under the microscope they are seen to correspond to laminated grainstones of peloids (Fig. 4.4f). The laminated appearance is related to the alternating grain size of the peloids and to the sparitic amount. Echinoderm fragments and ooids are secondary grains in this microfacies, though locally abundant in some beds. This lithofacies is recorded, mainly recorded in the Serpentinum, Bifrons and Gradata zones; yet the thickest level (IZ-24) is located in the Aalensis Zone (Fig. 4.5). In general the record of this lithofacies decreases throughout the section. The contact between the white laminated limestones and the red nodular limestone lithofacies is irregular and sharp.

4.1.3 Microfossil Assemblages

The microfossil assemblage is dominated by filaments, foraminifera and ostracods, but radiolaria and ammonitella are very abundant in the nodular limestones of the Aalensis Zone (Figs. 4.4 and 4.5).

Filaments are the most common microfossil, with a size ranging from 5 to 3 mm for complete valves, but they appear frequently as smaller fragments (Fig. 4.4b). The filaments are common both in nodular limestones and locally in the white laminated limestones, where they are oriented according to lamination. In nodular limestones, filaments are short fragments and they are locally well preserved in intraclasts and in nodules.

Foraminifera (Figs. 4.6 and 4.7) are dominated by agglutinated forms of Textulariina (62%), followed by calcitic perforated shells of Lagenina (24%), and other orders (Milionina, Spirillinina and Robertinina). However, the composition of foraminiferal assemblages is clearly different in the grey-yellow limestones, the red nodular limestones and the white laminated limestones. The red nodular limestones and grey-yellow limestones are dominated by Suborder Lagenina (43%), mainly uniserial forms (*Dentalina* and *Nodosaria*) and coiled forms (*Lenticulina*). Textulariina (41%) are dominated by biserial and triserial shells (*Verneuilinoides*, *Pseudomarsonella* and *Gaudryina* among others). Agglutinated coiled forms are locally important, with local abundances of *Glomospira* and *Meandrospira*. The foraminiferal assemblage from these lithofacies is completed with Spirillinina (9%), Milionina (2.5%), undifferentiated encrusters and Robertinina.

The foraminiferal assemblage from the white laminated limestones is clearly different, characterised with the highest values of Textulariina (81%) and Milionina (15%), as well as low values of Lagenina (4%). Spirillinina and Robertinina are not recorded in this lithofacies. The most abundant foraminifera are *Verneuilinoides*,

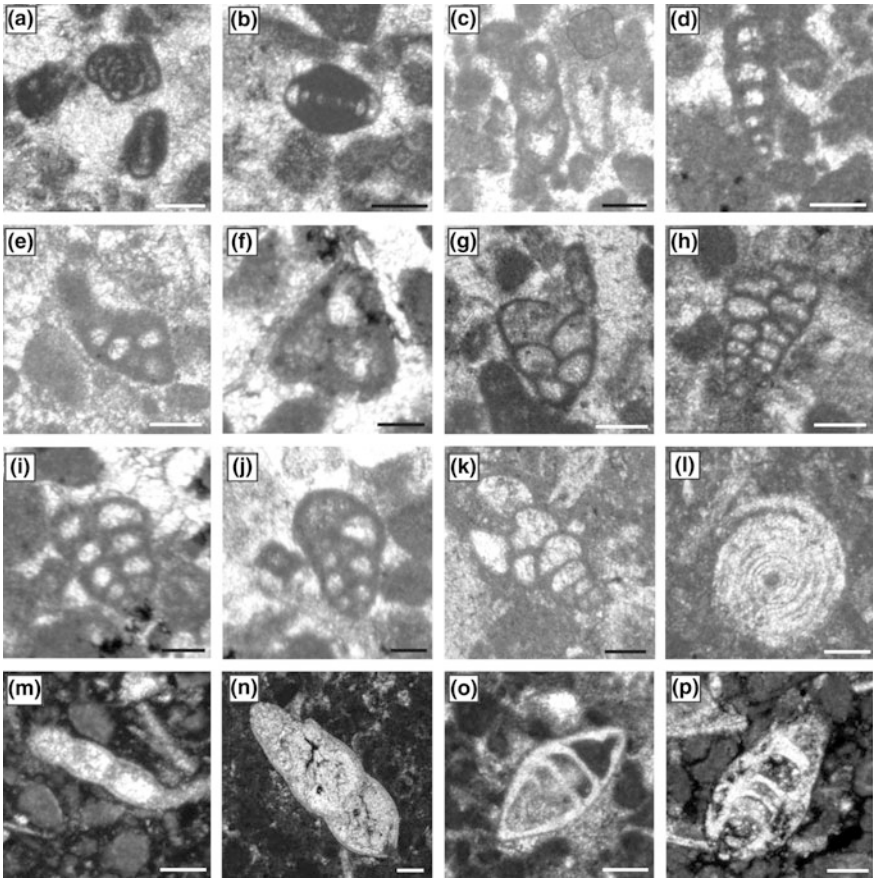

Fig. 4.6 Foraminifera from *thin* section. **a** *Glomospira* (*upper* specimen) and *Nautiloculina* (white laminated limestone, Serpentinum Zone). **b**. *Nautiloculina* (white laminated limestone, Serpentinum Zone). **c** *Ammobaculites* (white laminated limestone, Bifrons Zone). **d**. *Ammobaculites* (white laminated limestone, Aalensis Zone). **e** *Gaudryina heersumensis* (white laminated limestone, Bifrons Zone). **f** *Gaudryina heersumensis* (white laminated limestone, Aalensis Zone). **g** Biserial agglutinated foraminifera (white laminated limestone, Serpentinum Zone). **h** *Textularia* (white laminated limestone, Serpentinum Zone). **i** *Textularia* (white laminated limestone, Aalensis Zone). **j** *Verneuilinoides* (white laminated limestone, Aalensis Zone). **k** Verneuilinoid (white laminated limestone, base of Gradata Zone). **l** *Spirillina* (red nodular limestone, Gradata Zone). **m** *Nodosaria* (red nodular limestone, Reynesi Zone). **n** *Dentalina* like (red nodular limestone, Aalensis Zone). **o** *Lenticulina* (white laminated limestone, Bifrons Zone). **p** *Lenticulina* (red pseudonodular limestone, Reynesi Zone). Scale bar 100 μm

Gaudryina, *Glomospira*, *Pfenderina*, *Pseudomarsonella* and *Ophthalmidium*. Some of the genera recorded in the white laminated limestones are exclusively from shallow environments (e.g., *Paleopfenderina*, *Pseudomarsonella*, *Quinqueloculina* and *Nautiloculina*; see Helm 2005; Reolid et al. 2009; among others).

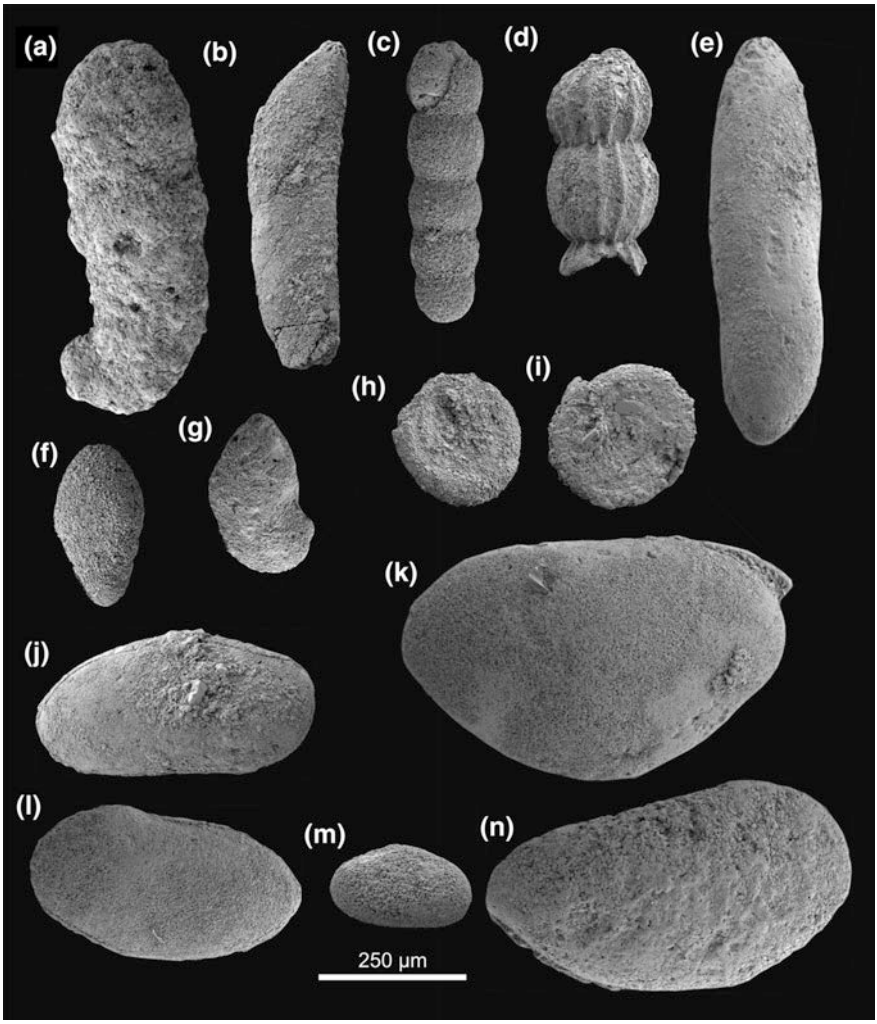

Fig. 4.7 Foraminifera and ostracods from sieved samples from Bifrons and Reysensi zones. **a** *Ammobaculites agglutinans* (Bifrons Zone). **b** *Dentalina* sp. (Bifrons Zone). **c** *Nodosaria* sp. (Reynesi Zone). **d** *Nodosaria fontinensis* (Bifrons Zone). **e** *Eoguttulina biloculari*s (?) (Reynesi Zone). **f** *Pseudonodosaria vulgata* (Reynesi Zone). **g** *Planularia* sp. (Bifrons Zone). **h** *Ammodiscus asper* (Reynesi Zone). **i** *Spirillina infima* (Reynesi Zone). **j** *Bairdiacypris rectangularis* (Bifrons Zone). **k** *Bairdia eirensis* (Bifrons Zone). **l** *Bairdiacypris triangularis* (Bifrons Zone). **m** *Pseudohealdia bispinosa* (Bifrons Zone). **n** *Bairdia molesta* (Bifrons Zone)

The stratigraphic distribution of foraminifera presents two maximum values of diversity represented by the number of genera, the first one in Bifrons Zone—after an increasing diversity trend from the base of the Toarcian—and the second one located in the Aalensis Zone, related to the input of shallow water foraminifera in a

white laminated limestone bed. The lowest values occur at the base of the section (Polymorphum Zone) and in the uppermost part of the Bifrons Zone. The highest proportions of foraminifera typical of shallow water environments are recorded in the lower part of the section, where white laminated limestones are more frequent, as well as in the bed IZ-24, which is a thick white laminated limestone within the ammonitico rosso facies of the Aalensis Zone.

Ostracods (Fig. 4.7) are common in the marls and marly limestones of the Bifrons Zone (second stratigraphic interval) and in the red nodular limestones of the Gradata Zone at the beginning of the third stratigraphic interval, and they are scarce in the white laminated limestones. Ostracods mainly correspond to Order Podocopina (superfamilies Bairdioidea and Pontocypridoidea)—with an abundance of *Bairdia*, *Bairdiacypris* and *Isobithocypris*; and secondarily *Liasina*, *Pontocyprella* and *Pseudomacrocypris*. Bairdioids dominate the ostracod assemblage.

Radiolarids are preserved as recrystallised moulds. They appear in the upper part of the Bifrons Zone and they are more frequent in the top of the section (Aalensis Zone) inside nodules. This situation has been also reported in Upper Jurassic red nodular limestones of the Subbetic (Comas et al. 1981).

Ammonitella are recorded from the lower part of the Bifrons Zone (second stratigraphic interval) and they are very common in the Aalensis Zone (Figs. 4.4c and 4.5). The mean size of the ammonitellas is 0.9 mm. These embryonic shells are preserved exclusively in nodules.

4.1.4 Trace Fossils

Trace fossil assemblages vary according to the studied lithofacies (Fig. 4.8). In grey-yellow limestones the trace fossils are hardly observed and they correspond to *Chondrites*, *Planolites* and *Thalassinoides*.

In the red nodular limestones (calcareous ammonitico rosso) and nodular marly limestones (marly ammonitico rosso), trace fossils are very abundant and densely distributed, with a record of *Chondrites*, *Phycodes*, *Planolites* and *Thalassinoides* (Fig. 4.8c, d) Subhorizontal trace fossils are dominant. *Chondrites* appear in all of the beds. In the case of the most nodular limestones with nodules with sharp edges, small *Chondrites* (1.5 mm in diameter) are restricted to clay-rich intranodules and are not found inside the calcareous-rich nodules. The largest trace fossils are mostly located at the base of the beds. In the case of *Phycodes* and *Planolites* they reach a maximum diameter of 7.3 mm, and *Thalassinoides* reaches 15.5 mm. Colour infilling of the trace fossils allows for discernment between red and white trace fossils in each surface; red infilling is recorded in *Phycodes*, *Chondrites* and *Thalassinoides*, whereas white infilling is observed mostly in *Planolites* and *Phycodes*. White infilling traces cross-cut red infilling structures.

In the white laminated limestones trace fossils (Fig. 4.8e, f) are located in the base of the beds. *Chondrites* are absent. *Planolites* and *Phycodes* are recorded, as well as *Ophiomorpha*, characterised by a well-developed pelleted mud lining. The

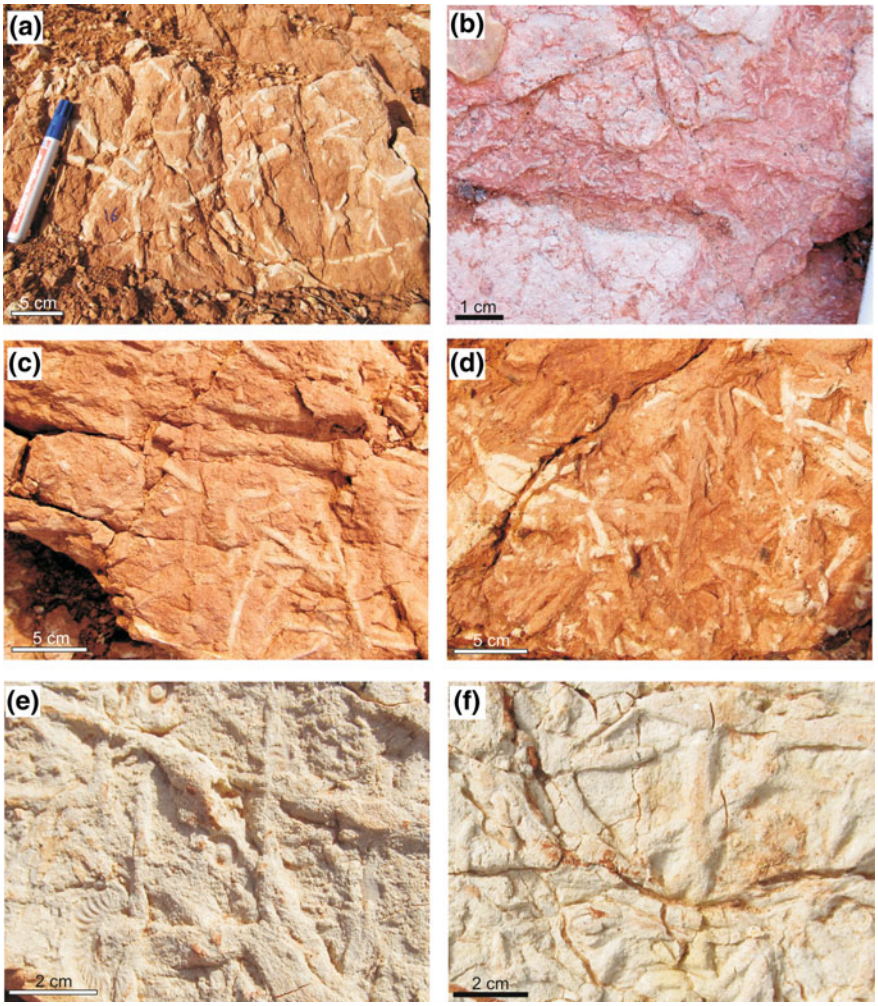

Fig. 4.8 Trace fossils. **a** *Planolites* from red nodular limestone (Gradata Zone, Middle Toarcian). **b** *Chondrites* mainly located in the matrix between nodules (Aalensis Zone, Upper Toarcian). **c** *Planolites* (white traces) and *Thalassinoides* (large red traces) from red nodular limestones (Gradata Zone, Middle Toarcian). **d** Dense burrowed base of red nodular limestone by *Phycodes* (Reynesi Zone, Upper Toarcian). **e** and **f** *Phycodes* and *Ophiomorpha* from white laminated limestone (Serpentinum Zone, Lower Toarcian)

maximum size is reached by *Ophiomorpha*, 6–8 cm in diameter. Different indeterminate trace fossils, in some cases showing a probable spreiten infilling, are common at the base of these beds. In some cases, external moulds of ammonoids have been recorded overprinting previously formed trace fossils.

4.1.5 Interpretation

Origin of sediment and lithofacies

The ammonitico rosso facies were associated with epioceanic slopes of a sedimentary swell-trough system related to the extensional phase of continental rifting. The Iznalloz section shows the progressive installation of ammonitico rosso facies during the Toarcian with an evolution to hemipelagic swells after the fragmentation of the carbonate platform. The hemipelagic swells are topographically high sea bottoms located in epi-oceanic environments, limited by faults (horst-graben systems or tilted blocks related to listric faults) and developed on continental crust containing condensed deposits (Santantonio 1993, 1994).

The record of well laminated limestones related to distal deposits of tempestites or turbidites within the marly interval and the ammonitico rosso facies would point to slope or foot-slope sedimentary environments. The presence of these beds could be related to the intensified storm events proposed by Krencker et al. (2015). These authors interpret an intensification of tropical cyclones during the Toarcian Oceanic Anoxic Event based on sections from West Europe and Morocco with inner to outer neritic settings represented. However, in the case of the Iznalloz section, and the Subbetic in general, this intensification of storm events during the Early Toarcian is not evident. The white laminated limestones are not restricted to or more abundant in Lower Toarcian, and they are recorded from Serpentinun to Aalensis zones. Other Subbetic sections such as Fuente Vidriera, La Cerradura and Colomera have not tempestite beds (e.g., Rodríguez-Tovar and Uchman 2010; Sandoval et al. 2012; Reolid et al. 2014b).

Carbonates and clay minerals are the main components of the studied lithofacies (Braga et al. 1981; Palomo 1987; Reolid et al. 2015). The pelagic character of the swells resulted in isolation or a poor connection with the emerged areas and the shallow platform. Hence, the input of sediment coming from these areas, including the carbonate factory, is severely reduced. The sedimentation is limited to the accumulation of planktic and nektonic organisms (calcareous nannoplankton, radiolarians, ammonites, nautiloids and belemnites) but probably affected by sediment winnowing by currents (Reolid et al. 2015).

Clay minerals (illite, smectite, chlorite and kaolinite; Palomo 1987) constitute the other important component, in this case allochthonous. The content of kaolinite is particularly interesting as a marker of continental runoff, indicative of palaeoclimatic conditions as well as of some incidence of pedogenesis and physico-chemical weathering in neighbouring emerged areas (e.g., Parisi et al. 1996; Dera et al. 2009; Hermoso and Pellenard 2014).

In terms of the benthic calcareous productivity, it is worth noting that the depth of this lithofacies was probably below the euphotic zone, due to the scarcity of benthic macroinvertebrates (crinoids and brachiopods recorded only locally). A depth within the euphotic zone could trigger carbonate production by primary photosynthetic organisms. However, the record of the white laminated limestones

with common oolites and foraminifera, typical of shallow water environments, suggests that the shallowest areas of the pelagic swell were within the shallow euphotic zone (*s*. Vogel et al. 1995). The white laminated limestones are distal deposits related to turbidites or tempestites with lamination in the base of the beds. Ichnological features support the turbiditic character of these lithofacies. *Phycodes* has been described as associated to turbiditic facies, usually preserved as convex hyporelief expressions of endorelief burrow systems on the soles (i.e., Han and Pickerill 1994; Gong 2001; Uchman and Tchoumatchenco 2003; Savrda 2012; Monaco and Trecci 2014). Thus, an abundance of *Phycodes* in the base of the white laminated limestone beds is compatible with the turbiditic deposition of these sediments; colonisation by *Phycodes* tracemaker was relatively immediate after deposition of the sandy interval, in a loose, unconsolidated substrate, as reflected by the deformation of *Phycodes* structures by deposition of ammonite carcasses.

Therefore, the white laminated limestones constitute allochthonous deposits but within this block of the Median Subbetic. The abundance of lumps and intraclasts in the other lithofacies—such as grey-yellow limestones, mainly in red nodular limestones and marly limestones—is also congruent with the transport according to the slope of a tilted block. The thin-shelled bivalves are common in the studied lithofacies, and they present different fragmentation degrees; but well-preserved shells of these delicate organisms are commonly recorded, probably being autochthonous or para-autochthonous.

In the Gradata Zone (Middle Toarcian), the ammonitico rosso facies debut (red nodular limestones and marly-limestones rich in trace fossils *Phycodes*, *Planolites*, *Thalassinoides* and *Chondrites*). Progressively more pelagic conditions and a restricted connection with emerged lands and carbonate platforms are reflected by the decrease in sedimentation rate, lesser input of turbidite-tempestite sediments (white laminated limestones) and increase of ammonitellas and radiolarids. The combined action of burrowing, compaction and dissolution controlled nodulation, which ranges from diffuse nodules to sharp edge nodules (Reolid et al. 2015). The sedimentation rate conditioned the time available for nodule growth, the migration of the Ca^{2+} and HCO^{3-} precipitation horizon, and the nodulation degree (from horizons with diffuse edge nodules or semicontinuous to continuous layers formed by the coalescence of sharp edge nodules) (Fig. 4.9). Nodules are mainly composed by calcite whereas internodule areas are enriched in clay minerals as evidenced by X-ray microfluorescence mapping of elements (Fig. 4.9).

The differentiation between clay- and carbonate-rich areas within the sediment, in association with nodulation, is also favoured by burrowing (e.g., Fürsich 1973, 1979; Eller 1981; Reolid et al. 2015). Given the abundance of burrows in the nodular limestones of the Iznalloz section, it is evident that the activity of burrowers enhanced sediment permeability and porewater circulation, and thus the dissolution-reprecipitation processes.

The composition and richness of trace fossils from the calcareous ammonitico rosso and nodular marly limestones agree with the influence of bioturbation on nodular appearance. *Thalassinoides* has been frequently associated with ammonitico rosso facies and nodularity, reflecting greater substrate consistency during

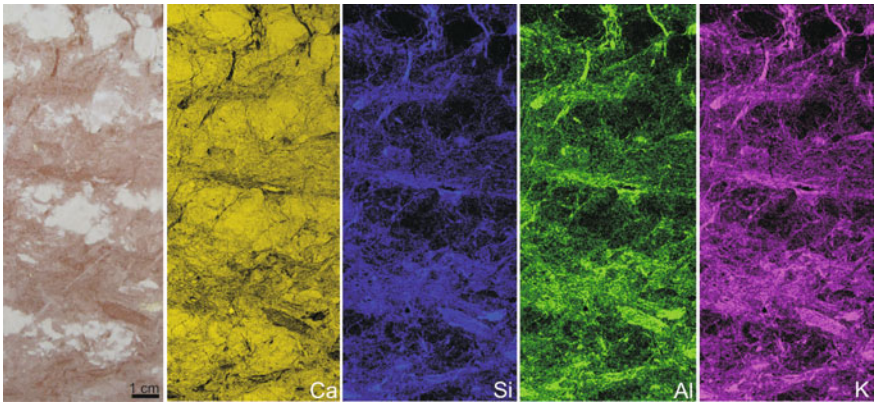

Fig. 4.9 Polished slab of red nodular limestone of the Upper Toarcian from Iznalloz section and X-ray microfluorescence compositional maps for Ca, Si, Al and K. See the white nodules correspond to Ca-rich areas (calcite), and red internodules correspond to areas comparatively rich in Si, Al and K (higher concentration of clays)

colonisation; for this reason it is used as a tool to evaluate sedimentation rates, minor erosions, discontinuities, or stratigraphic completeness, including examples from the Betic Cordillera (i.e., Caracuel et al. 1997, 2000; Monaco et al. 2007; Rodríguez-Tovar and Nieto 2013; Nieto et al. 2014). The abundance of burrows at the base of some calcareous beds from Gradata to Aalensis zones indicates pauses in deposition with minor or no erosion (omission surfaces, e.g., IZ-14, IZ-15, IZ-22, IZ-25, IZ-26), which is normal in a context of low sedimentation rate (e.g., Kennedy and Garrison 1975; Fürsich 1979; Braga et al. 1981; Reolid et al. 2010). In the Iznalloz section, differences in trace fossil composition and fossil infilling colour observed in the red nodular limestones—red infilling mainly in *Phycodes*, *Chondrites* and *Thalassinoides* and white infilling mostly in *Planolites* and *Phycodes*—could be related to two episodes of colonisation, reflecting the activity of two different communities, with minor erosion in between. During deposition of the red nodular limestone, a coetaneous red infilling trace fossil assemblage is emplaced. *Chondrites*, mostly associated to internodule sediment, reveal a less cohesive substrate, richer in organic matter than the one corresponding to the nodules. Later, during the deposition of white sediments, a white infilling trace fossil assemblage cross-cuts the previous one. These two successive communities must have been replaced in a short time, without significant environmental changes. The white laminated limestones are, in general, poorly developed in the nodular facies and support the interpretation of a short time deposition and/or minor erosion of the white sediments.

In comparison with ammonitico rosso facies, the trace fossils from the white laminated limestones indicate that these peloidal deposits constituted a loose-ground. This is also in agreement with the record of *Ophiomorpha*.

Oxygenation

In general terms, ichnofossil and microfossil assemblages (foraminifera, ostracoda and echinoderm fragments) recorded in the Iznalloz section indicate good oxygenation in the sea-bottom. The abundance of ammonoids, as well as the record of belemnites, also indicates good oxygen conditions in the water column.

Trace fossil composition and abundance are indicative of the good oxygenation degree, both in white laminated limestones and in ammonitico rosso facies. Trace fossils (*Chondrites*, *Planolites* and *Thalassinoides*) are less common and poorly observed in grey-yellow limestones of the Lower Toarcian.

In the ammonitico rosso facies, the *Phycodes* dominated assemblage reveals a predominance of deposit-feeders, probable tracemakers being vermiform annelids and crustaceans. In this context of oxygen availability, the diversity of behaviours (*Phycodes* fodinichnia, *Chondrites* chemichnia, *Thalassinoides* domichnia-fodinichnia, and *Planolites* pascichnia) reveals food content availability at the sea-bottom.

The foraminiferal assemblage of the white laminated limestone also indicates good oxygen availability in the source area, surely in shallower environments, due to the allochthonous character of these turbidites or tempestites.

In autochthonous lithofacies (grey-yellow limestones, grey-red marls and red nodular limestones and marly limestones) the foraminifera are well represented from potential deep infaunal forms (e.g., *Eoguttulina*, *Lenticulina*, *Verneuilinoides* and *Reophax*) to shallow infaunal (e.g., *Ammobaculites*, *Astacolus*, *Dentalina*, *Marginulina*, *Nodosaria*) and epifaunal forms (e.g., *Glomospira*, *Ophthalmidium*, *Spirillina, Trochammina*). This is clearly related to a high degree of oxygenation (e.g., Reolid et al. 2008; Olóriz et al. 2012). The dense burrowing favoured the oxygenation of the infaunal microhabitats of foraminifera.

The absence of the dark interval that typically characterises oxygen restricted biofacies with preservation of organic matter related to the Toarcian Oceanic Anoxic Event (as evidenced in External Subbetic sections such as La Cerradura, Cueva del Agua and Fuente Vidriera), would confirm the oxygen availability in the sea-bottom. These deposits, mainly the ammonitico rosso facies, are reddish due to the slow sedimentation under fully oxidizing conditions (e.g., Jenkyns 1971). According to Hallam (1967) and Berner (1969), the red colour is related to diagenetic alteration of goethite to hematite.

The physiography of the bottom in this setting during the Toarcian—evolving to pelagic swell affected by currents—was unfavourable to water stagnation and oxygen depleted conditions. However, these adverse conditions for benthic assemblages were recorded in comparatively deeper parts (subsident troughs) of the Subbetic dominated by expanded successions with marl-limestone rhythmites and dark marls (Reolid et al. 2013b, 2014b; Rodríguez-Tovar and Reolid 2013; Reolid 2014). In addition, oxygenation was favoured by the tempestite-turbidite imputs to the bottom waters during the Early Toarcian. In the Polymorphum and Serpentinum zones, the foraminiferal assemblages confirm good oxygenation with no dominance of opportunists such as *Lenticulina*, *Reinholdella* and *Eoguttulina* (Reolid et al. 2012a, b, 2014a; Reolid 2014; Rita et al. 2016).

Nutrient content

In the context of oxygen availability, a diversity of feeding behaviours reveals food content availability at the substrate. *Phycodes* has been related to a variety of behavioural activities, usually linked to the means of exploiting nutrient-rich sediments (Han and Pickerill 1994; Mángano et al. 2005). Complex *Thalassinoides-Phycodes* compound burrows have been related to dwelling-deposit feeding structures operating for relatively long intervals; reburrowing by *Chondrites* is associated with storage of organic material or feces and cultivating bacteria, as a behaviour that supplements deposit feeding (Miller 2001). As previously commented, the presence of *Chondrites* mostly associated to internodule sediment could reflect a comparatively higher abundance of organic material in the internodule substrate.

The diversity of benthic foraminifera confirms nutrient availability throughout the section, but not high values, probably owing to the hemipelagic context. The highest diversity values are related to allochthonous deposits, represented by the white laminated limestones, where foraminifera with epifaunal/epiphytal behaviour (*Ammodiscus*, *Glomospira*, *Meandrospira*, *Nautiloculina*, *Trochammina*, *Ophthalmidium*, *Quinqueloculina*, *Spirillina* and *Conicospirillina*) reach maximum values. These fauna come from a shallow environment with high productivity and water energy, where bacterial scavengers, phytodetritivores, grazing herbivores and primary weed fauna proliferate (e.g., Reolid et al. 2013a).

In the grey-yellow limestones, grey and red marls and red nodular limestones, the Suborder Lagenina dominates the foraminiferal assemblage, with shallow to deep infaunal forms being active deposit feeders, bacterial scavengers and grazing omnivores (mainly *Astacolus*, *Dentalina*, *Lenticulina*, *Nodosaria* and *Marginulina*); epifaunal grazing herbivores are represented by scarce *Spirillina*, *Epistomina* and *Trochammina* (Reolid et al. 2013a, 2014a). In these lithofacies, foraminiferal assemblages indicate that nutrients were exploited mainly in the infaunal microhabitat for foraminifera, perhaps related to the byproducts (fecal matter and mucous excretions for burrow stabilisation *s*. Petrash et al. 2010) of macroinvertebrate burrowers.

Palaeoenvironmental reconstruction

The evolution of the Central Median Subbetic in this area is mainly controlled by the rupture of the Lower Jurassic shelf during the late Pliensbachian (Vera 1988), in a scenario resembling other Tethyan Domains recorded in the Western Alps (Dercourt et al. 1985; Funk et al. 1987), Southern Alps (Bosellini 1973; Winterer and Bosellini 1981), Apennines (D'Argenio 1974; Cecca et al. 1992; Parisi et al. 1996), western Slovenia (Rozic and Smuc 2011), Rif Cordillera (El Kadiri 2002), Traras Mountains (Marok and Reolid 2012), Saharian Atlas (Elmi and Almeras 1984; Yelles-Chaouche et al. 2001), High Atlas of Morocco (Ettaki et al. 2000; Ettaki and Chellaï 2005), and the Central Atlas of Tunisia (Soussi and Ben Ismail 2000; Soussi et al. 2000). The diversified physiography of the Subbetic basin during the Toarcian, related to synsedimentary tectonic activity and circulation patterns,

probably determined different intensities of ventilation conditions on the sea-floor. As happens in other areas of the southern Tethys, such as Apulia and the North African Margin, the Toarcian deposits overlie basinal pelagic limestones containing cherts as well as thick hemipelagic marly-limestone sequences (e.g., Marok and Reolid 2012). The Early Toarcian transgression (Haq et al. 1987; Hallam 1988, 2001) does not indicate the drowning of carbonate platforms because it usually overlies hemipelagic deposits of the upper Pliensbachian. Progressive fragmentation of the Lower Jurassic platform is even reflected by the input of turbidites or tempestites in the first and second stratigraphic intervals (mainly Serpentinum and Bifrons zones), represented by the white laminated limestones consisting almost exclusively of peloids, thin-shelled bivalves and shallow foraminifera. These turbidites were originated from fragmented drowned platform margins and subsequently redeposited along slopes of the tilted blocks. Therefore, the intercalations of white laminated limestones reflect regionally recognised events that characterised the sedimentary evolution of the Median Subbetic at the end of the Early Jurassic. The record of slumps in nearby areas of the Median Subbetic (e.g., Colomera section, 15 km west) reflects uneven sea-bottom palaeotopography that originated during an early to middle Toarcian phase of accelerated subsidence. The Lower Toarcian clay mineral association (illite, smectite, chlorite, *s*. Palomo 1987) is characteristic of a hemipelagic environment with a low influence of emerged reliefs. Given the transgressive context of the Early Toarcian (Haq et al. 1987; Hallam 2001) the source area of the clays (emerged land) was comparatively far away.

During the Middle and Late Toarcian the pelagic swell became fully installed in epi-oceanic conditions. The progressively more reddish facies show increasing contents in kaolinite and nodularity, and a less common record of white laminated limestones. The second stratigraphic interval is a marly ammonitico rosso, while the third stratigraphic interval increases in carbonate content and in the record of omission surfaces, resulting in calcareous ammonitico rosso (increasing nodulation toward the top of the section). A progressively higher condensation degree in the section can be deduced from these facies changes. However, this higher condensation for ammonitico rosso facies is not justified in this section. Stratigraphic condensation (as well as the presence of expanded sections) should be measured on the basis of thickness for a given (the same) time interval (i.e., Gómez and Fernández-López 1994) reflecting on this way the sedimentation rate. Within the Iznalloz section, the Polymorphum Zone is much thinner than any other biozone of the section but this is affected by the hiatuses located in the Pliensbachian-Toarcian boundary and in the Polymorphum-Serpentinum zone boundary also recorded in other sections of the Subbetic (e.g., Nieto et al. 2008; Reolid et al. 2014b). The Serpentinum Zone has duration of 1.08 Ma for Ogg and Hinnov (2012), 1.5–1.62 Ma for Boulila et al. (2014) and 1.31 Ma for Ruebsam et al. (2014) and is 2.62 m-thick, but is not represented by ammonitico rosso facies (sedimentation rate ranging from 0.24–0.16 cm/kyr). The Aalensis Zone, represented by ammonitico rosso facies is 3.00 m-thick for a duration of 1 Ma in Gradstein et al. (2004), 0.13 Ma for Ogg and Hinnov (2012) and 0.44–0.51 Ma in Boulila et al. (2014) (2.3–0.59 cm/kyr), so it can be said that is relatively expanded respect to the

Serpentinum Zone, but represented by the supposed condensed ammonitico rosso facies. There is not necessarily a univocal relationship between condensation and ammonitico rosso facies.

Estimations of sedimentation rate are of limited value because much of the time involved in the deposition of the red nodular limestones is represented by ubiquitous omission surfaces (Reolid et al. 2015) and the alluded disagreement of the proposals of duration for the different zones of the Toarcian Stage. However, it seems that sedimentation rate is not the main controlling factor for developing ammonitico rosso facies. The installation of pelagic swell in this area of the Subbetic, entailing isolation from sediment sources (emerged areas and carbonate factory represented by the Prebetic shelf) as well as the sea-level fall during the Middle-Late Toarcian (e.g., Hallam 1988, 2001), came to favour the sediment-winnowing by currents and seawater circulation in the uppermost sediment column, triggering early marine lithification and the subsequent nodulation. An increasing pelagic influence is signalled by the abundance of radiolarids and ammonitellas in the most calcareous ammonitico rosso.

The increase of kaolinite just in the third stratigraphic interval does not fit the trends described by Dera et al. (2009). These authors point to a kaolinite enrichment during Falciferum and Bifrons zones, and a decrease in kaolinite content during the Late Toarcian. These trends are held to be related to a warm climate with efficient runoff during the Falciferum and Bifrons zones, with cooler and drier climate during the Late Toarcian, mainly in northern parts of the Peritethyan Realm (Dera et al. 2009, 2011). In contrast, Reolid et al. (2015) interpret the absence of kaolinite during the Early Toarcian in the Median Subbetic as being related to high sea-level and relatively great distances to emerged lands; meanwhile, increasing values of kaolinite related to ammonitico rosso facies resulted from a low sea-level, favouring emersion of Subbetic islands. A latitudinal climatic zonation is envisaged, and the weathering and hydrolysis of emerged lands during Late Toarcian was possible in southern Tethys margins, despite the cooler conditions interpreted by other authors (e.g., Dera et al. 2009, 2011). According to Cecca et al. (1992), the Toarcian ammonitico rosso facies occurred between 15° and 30° N latitude, and it is widespread in the Mediterranean Tethys of the North Gondwana Palaeomargin (Apulian promontory and North African Margin) and the southern Iberian Palaeomargin (Betic Cordillera). The kaolinite-rich association of the Middle and Upper Toarcian must have been deposited under the influence of nearby emerged areas (perhaps Subbetic islands), as shown by the greater abundance of kaolinite and the decrease of smectite.

4.2 Arroyo Mingarrón Section

The Arroyo Mingarrón section is located in the Granada Province, 1 km northeast to the Colomera village, in front of the village, in the Mingarrón ravine (37° 22′ 54.33″ N; 3° 42′ 27.18″ W; Figs. 3.1 and 4.10). An additional section is observed in

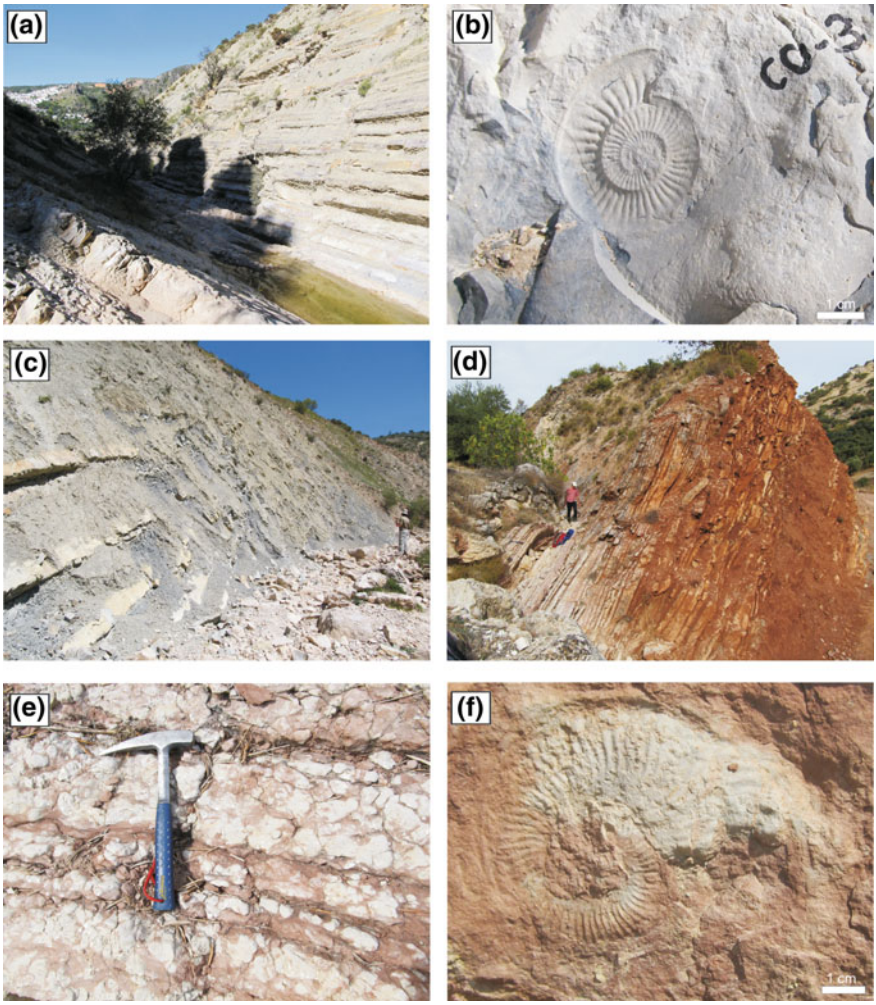

Fig. 4.10 Field view of the Arroyo Mingarrón section. **a** Yellowish marl and limestone alternance of the Uppermost Pliensbachian-Lower Toarcian (Polymorphum Zone). **b** Ammonite mould (*Canavaria*) in the uppermost Pliensbachian. **c** marls of the Lower Toarcian (Serpentinum Zone) to Middle Toarcian (Bifrons Zone). **d** Marly to calcareous ammonitico rosso facies of the Upper Toarcian. **e** Detail of the calcareous ammonitico rosso with sharp edge nodules. **f** Ammonite mould (*Pseudogrammoceras*) from the ammonitico rosso facies (Upper Toarcian)

the Colomera Village, from threshing floors to the Roman Bridge over the Colomera River (Fig. 4.11).

The Arroyo Mingarrón section, as well as the Colomera section, shows the progressive development of the ammonitico rosso facies during the Toarcian with

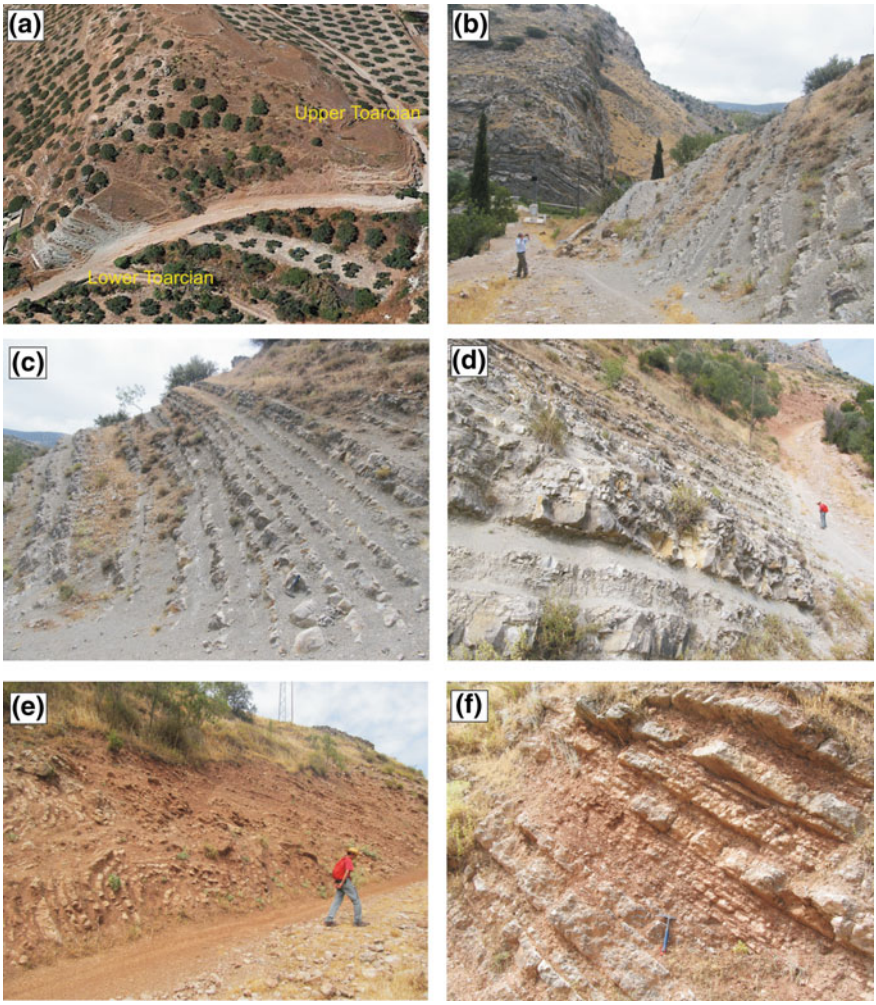

Fig. 4.11 Field view of the Colomera section. **a** Perspective from the blue-greish marl-limestone rhythmite of the uppermost Pliensbachian-Lower Toarcian to red ammonitoco rosso facies of the Upper Toarcian (view from Google Earth). **b** Blue-greish marl-limestone rhythmite of the uppermost Pliensbachian-Lower Toarcian, the relief in the bottom corresponds to the Pliensbachian cherty limestones. **c** Blue-greish marls and limestones rhythmite of the Lower Toarcian. **d** Blue-greish marls and limestones rhythmite of the Lower Toarcian and red ammonitico rosso marls and nodular limestones in the upper part. **e** Slumps affecting the red marls and limestones of the Middle Toarcian. **f** The upper part of the Colomera sections is more calcareous and nodular (Upper Toarcian)

the onset of a hemipelagic swell. The analysis of the Arroyo Mingarrón section focused on the analysis of lithofacies and microfacies with a biostratigraphic control provided by calcareous nannofossils.

4.2.1 Lithofacies and Microfacies

The study section starts with a lower stratigraphic interval composed by yellowish marl-limestone alternances (11.3 m thick, Fig. 4.10a, b) developed over the cherty limestones of the Pliensbachian (Gavilán Fm). The lower part of this interval is characterised by ammonites of the genera *Emaciaticeras* and *Canavaria* (beds CO-1 to CO-30; Fig. 4.10b), while the upper part presents *Protogrammoceras* and *Dactylioceras*. The microfacies is characterised by peloidal mudstones to wackestones (Fig. 4.12a).

The second stratigraphic interval (42.8 m thick) consists of blue-greyish marls with scarce marly-limestone interlayers (Fig. 4.10c). Ammonites are scarce and poorly preserved. Trace fossils are close to those described in La Cerradura section, with dominance of *Planolites*. Clay content is high with dominance of illite and smectite, and chlorite.

The third stratigraphic interval (10.1 m thick) is constituted of reddish pseudo-nodular marls and marly-limestones (Fig. 4.10d). They are marly ammonitico rosso facies like those described in the Iznalloz section, but trace fossils are less common and poorly preserved compared to those of the Iznalloz section. These facies progressively change to red nodular limestones, the calcareous ammonitico rosso facies (Fig. 4.10e). The boundary between nodules and internodules is well-marked by the colour change, white nodules and red internodules. The largest nodules (3–5 cm) are located in the upper part of the section and they present spheroidal shape with the sharp edges usually in contact with stylolites forming more or less continuous nodular horizons. Trace fossils are scarcer than in the ammonitico rosso facies from Iznalloz section and they are represented mainly by *Thalassinoides*. *Phycodes* and *Chondrites* were not recorded whereas they are highly abundant in the Iznalloz section. The microfacies are packstones of peloids, filaments and ammonitella (Fig. 4.12b–d). Kaolinite content increases in this stratigraphic interval as occurs in the Iznalloz section.

The complementary Colomera section (Fig. 4.11) differs respect to the Arroyo Mingarrón section in the second stratigraphic interval here represented by a blue-greyish marls with abundant marly-limestone interlayers (24 m thick). This is thinner and with more carbonate than in the Arroyo Mingarrón section. The third stratigraphic interval in the Colomera section is represented by marly ammonitico rosso facies with *Thalassinoides* and *Zoophycos*, affected by slumps (39 m thick). The top of the section consists of 10 m of calcareous ammonitico rosso facies similar to those described in the Iznalloz and Arroyo Mingarrón sections, but locally with high amount of *Zoophycos*.

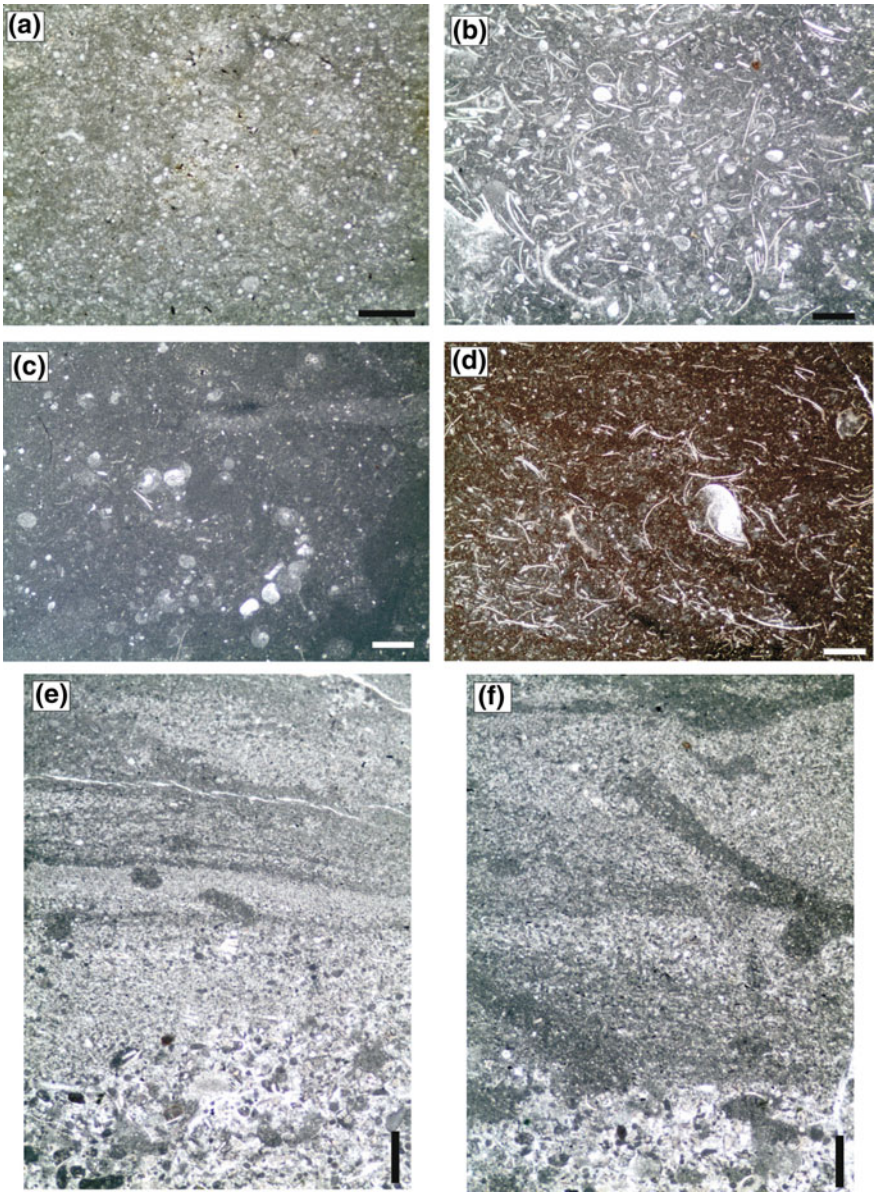
(a)
(b)
(c)
(d)
(e)
(f)

◂**Fig. 4.12** Most significant microfacies from Arroyo Mingarrón section. **a** Wackestone of radiolarians (yellowish marl-limestone alternance, NJT 5b nannofossil Subzone, uppermost Pliensbachian). **b** Wackestone-packstone of filaments and ostracods (calcareous ammonitico rosso facies, NJT 7b nannofossil Subzone, Upper Toarcian). **c** Wackestone of ammonitella (marl-limestone rhythmite, NJT 7a nannofossil Subzone, Middle Toarcian). **d** Packstone fo filaments and peloids (calcareous ammonitico rosso facies, NJT 7b nannofossil Subzone, Upper Toarcian). **e** Packstone of lumps and peloids with thinning upward trend (blue greish marls, NJT 6 nannofossil Zone, Lower Toarcian) and incipient lamination. **f** Packstone of lumps and peloids with thinning upward trend and small trace fossils of *Chondrites* (blue greish marls, NJT 6 nannofossil Zone, Lower Toarcian). Scale bar 1 mm

4.2.2 Calcareous Nannofossil

Both coccoliths and the *incertae sedis* nannolith *Schizosphaerella* are in general poorly to very poorly preserved in the Arroyo Mingarrón section, with exception of a few samples (Figs. 4.13 and 4.14). Severely overgrown specimens of *Schizosphaerella*, with development of secondary fringes, and of *Mitrolithus jansae* are commonly recorded. In spite of this poor preservation, almost all the samples are productive, although nannofossil abundance is low. Assemblages are largely dominated by *Schizosphaerella* and *M. jansae* in the Upper Pliensbachian and Lower Toarcian, by *Schizosphaerella* and *Lotharingius* species (mainly *L. hauffii* and *L. frodoi*) in the upper part of Lower Toarcian and Middle Toarcian, and by *Carinolithus superbus* and *Discorhabdus* (*D. ignotus* and *D. striatus*) in the Middle Toarcian and at the base of the Upper Toarcian. This assemblage indicates a south-Tethyan affinity for the Arroyo Mingarrón section.

Some first occurrences (FO) and one last occurrence (LO) of coccolith species allow dating the section according to the biozonation scheme of Mattioli and Erba (1999) created for the south-Tethyan region. The assemblage at the base of the section is latest Pliensbachian in age and belongs to the NJT 5a nannofossil subzone (Mattioli and Erba 1999). In sample CO-11, the FO of *Lotharingius sigillatus* is recorded, marking the base of the NJT 5b subzone. Although Mattioli and Erba (1999) reported this subzone at the base of the Toarcian, a recent study (Mattioli et al. 2013) shows that it encapsulates the Pliensbachian/Toarcian boundary as *L. sigillatus* first occurs in the latest Pliensbachian Emaciatum ammonite Zone in the Peniche GSSP section. Because in this last reference section the FOs of *Biscutum intermedium* and *Lotharingius* aff. *L. velatus* did occur at the very end of Pliensbachian (Oliveira et al. 2007; Mattioli et al. 2013), we tentatively place the Pliensbachian/Toarcian boundary slightly above these FOs, between samples CO-30 and CO-31.

The contemporaneous FOs of *Carinolithus superbus* and *C. poulnabronei* allow placing the base of the NJT 6 in the sample CO-48. This is the first sample of the blue-greyish marls that compound the second stratigraphic interval. This datum is very significant because the Early Toarcian Anoxic Event (T-OAE) is consistently recorded within the NJT 6 (Mattioli et al. 2004). Another relevant event is the LO of *Mitrolithus jansae* in the sample CO-78, that is usually recorded at the end of the

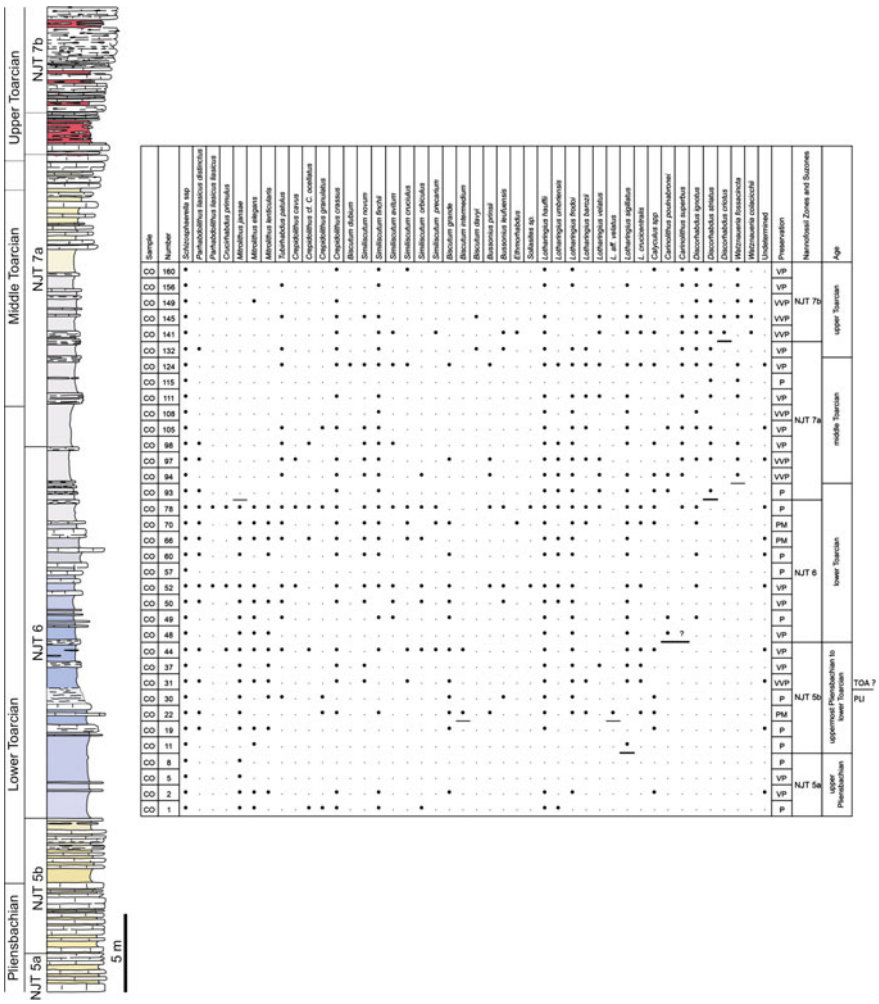

Fig. 4.13 Distribution of species of calcareous nannofossils recorded in Arroyo Mingarron section, nannofossil zones and general preservation of assemblages. Classification of nannofossils by Prof. Emanuela Mattioli (Univ. Lyon)

T-OAE (Mattioli et al. 2004). The top of the NJT 6 zone is marked by the FO of *Discorhabdus striatus* (sample CO-93, NJT 7a subzone) closely followed by the FO of *Watznaueria fossacincta* (small specimens, sample CO-94). The NJT 7a subzone spans the uppermost part of Lower Toarcian and the Middle Toarcian (Mattioli and Erba 1999). *Discorhabdus criotus*, which usually first occurs at the base of the Upper Toarcian, marks the base of the NJT 7b subzone (sample CO-141). The ammonitico rosso facies of the upper part of the Arroyo Mingarrón section would thus correspond to the base of Upper Toarcian.

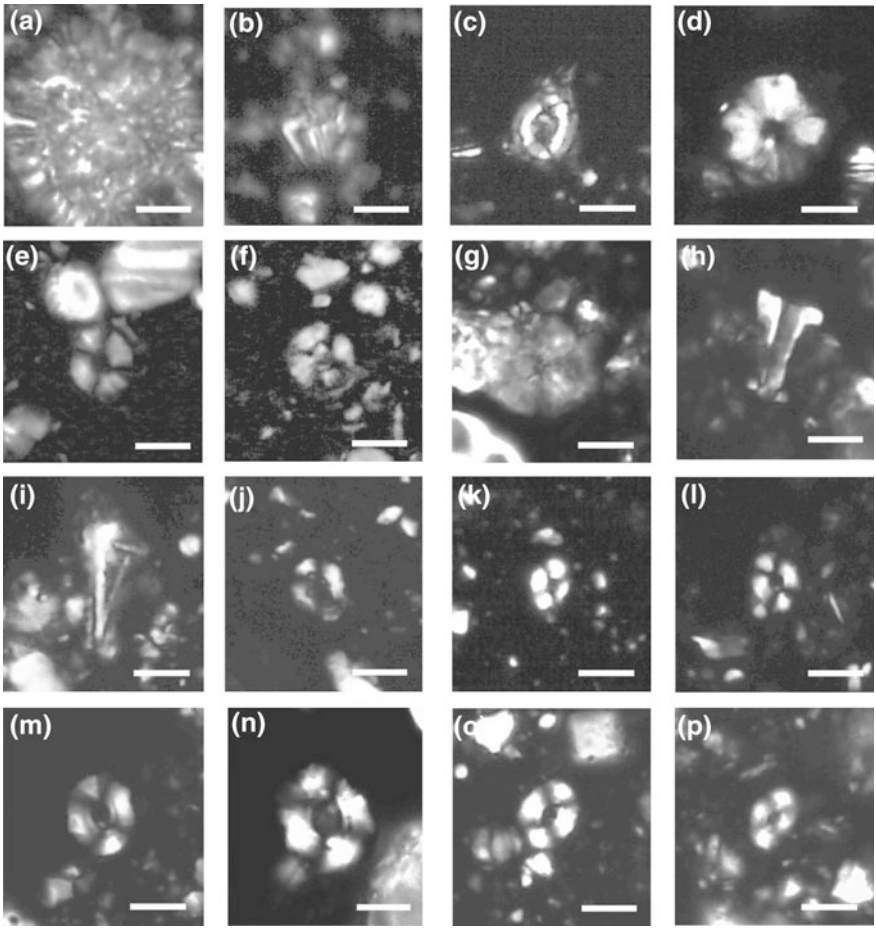

Fig. 4.14 Most significant calcareous nannofossils recorded in Arroyo Mingarrón section. Pictures by Prof. Emanuela Mattioli (Univ. Lyon). **a** *Schizosphaerella* spp. **b** *Mitrolithus jansae*. **c** *Tubirahbdus patulus*. **d** *Calyculus* spp. **e** *Similiscutum finchii*. **f** *Discorhabdus striatus*. **g** *Discorhabdus criotus.* **h** *Carinolithus poulnabronei*. **i** *Carinolithus superbus*. **j** *Bussonius leufuensis*. **k** *Lotharingius frodoi.* **l** *Lotharingius sigillatus.* **m** *Lotharingius crucicentralis.* **n** *Lotharingius velatus.* **o** *Watznaueria colacicchii*. **p** *Watznaueria fossacincta*. Scale bar 5 μm

4.2.3 Geochemistry

The analysis of geochemical proxies for palaeoproductivity, redox conditions, and detritism does not show significant trends in the Arroyo Mingarrón section. The yellowish marl-limestone alternance (NJT 5a and NJT 5b zones) displays an increasing trend of the TOC from 0.1 to 0.3 wt%. The $\delta^{13}C$ ranges between 0.45 and 0.89‰, and $\delta^{18}O$ ranges between −2.73 and −3.23‰.

The lower part of the blue-greyish marls (NJT 6 Zone) shows a progressive increase of $\delta^{13}C$ except for the decrease from 1.47 to 0.80‰ (a slight negative excursion of −0.77‰) coincident with the lowest diversity values of calcareous nannoplankton (Fig. 4.15). This is also coincident with the highest values of the Mg/Al ratio (a fluvial detrital proxy according to Chester et al. 1977). The lowest values of $CaCO_3$ content (26 wt%) together with the highest values of TOC (0.32 wt%) are recorded in the upper part of the NJT 6 Zone, 10 m above the minimum values of the calcareous nannoplankton diversity.

The upper part of the blue-greyish marls, corresponding to the NJT 7a Zone, evidences an increasing carbonate content (Fig. 4.15). The highest values of $\delta^{13}C$ are recorded at the beginning of this zone (3.08‰) and subsequently decrease to the top (1.74‰). The $\delta^{18}O$ does not change and keeps values around −2‰. The TOC values are very low (from 0.23 to 0.09 wt%). The Total Sulphur curve describes the same trends as the TOC. The lowest values from Arroyo Mingarrón section for Mg/Al ratio are recorded at the top of the NJT 7a.

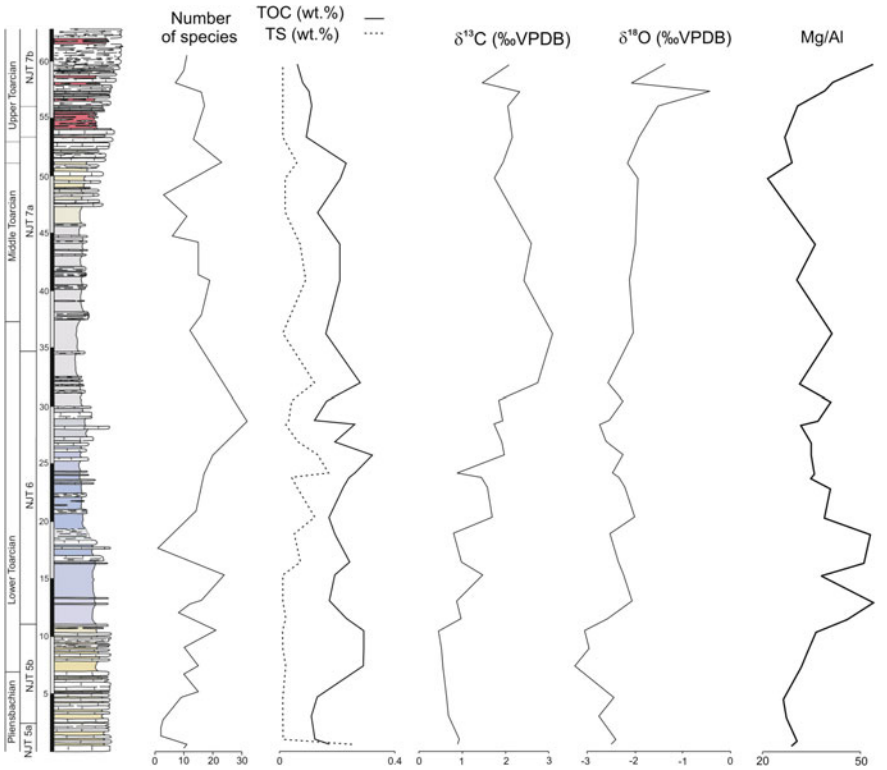

Fig. 4.15 Stratigraphic distribution of the diversity of calcareous nannoplankton (number of species), total organic carbon (TOC), total sulphur (TS), $\delta^{13}C$, $\delta^{18}O$ and the detrital proxy (Mg/Al ratio). The redox and palaeoproductivity proxies are not represented because there is not a stratigraphic trend

The reddish marly-limestones and pseudo-nodular limestones (NJT 7b Zone) experiment an abrupt increase in $CaCO_3$ and Mg/Al ratio. The organic matter content is extremely low (0.10–0.06 wt%). A positive excursion of the $\delta^{18}O$ occurs (reaching −0.42‰).

Taking into account the geochemical data and trends, it is difficult to locate the position of the T-OAE due to the absence of a clear negative carbon isotopic excursion. Moreover, the redox proxies, TS and TOC do not correspond to oxygen depleted conditions. Only the minimum values of nannoplankton diversity in the lower part of the blue-greyish marls of the NJT 6 Zone with decreasing $CaCO_3$, slight $\delta^{13}C$ fluctuations, and increasing Mg/Al ratio could indicate environmental changes during the early Toarcian.

4.2.4 Interpretation

The Toarcian Ammonitico Rosso context

The ammonitico rosso that characterises part of the Tethyan Jurassic has been interpreted as deposited at significant distance from a major continental landmass (e.g., Hallam 1967; Jenkyns 1971; Braga et al. 1981; Cecca et al. 1992). Deposition of the study sedimentary succession took place on the slopes of a sedimentary swell-trough system developed in the Subbetic during the Late Pliensbachian, with a maximum development during the Toarcian (e.g., Braga et al. 1981; Vera 1988; Reolid et al. 2015). The pelagic swells were common during the Jurassic in the Tethys Domain, being related to an extensional phase of the continental rifting and controlled by tectonic subsidence (e.g., Cecca et al. 1992; Santantonio 1994). The main evidence underlying this interpretation for ammonitico rosso facies from the Subbetic is the thickness variability of the Toarcian deposits between different sections (e.g., Iznalloz, Colomera, Arroyo Mingarrón, and La Cerradura) together with facies changes, in close space-time spans (e.g., Braga et al. 1981; Sandoval et al. 2012; Reolid et al. 2014b). The pelagic character of the swells results in isolation or a poor connection with the emerged areas and the shallow platform. Hence, the input of sediment coming from these areas, including the carbonate factory, is severely reduced. Moreover, due to the fact that the pelagic swells are topographic high at the sea bottom, sediment transport by bottom currents is also limited (Fig. 4.16). The sedimentation is restricted to the rain of calcareous nannoplankton and radiolarian carcasses, as well as the accumulation of cephalopod shells (mainly ammonites and secondarily nautiloids and belemnites). In the nodular limestones, however, the calcareous nannoplankton is relatively scarce compared with other sections of the Subbetic made up of marl-limestone rhythmites (Reolid et al. 2014b; Mattioli pers. commun.). This could be interpreted as sediment winnowing by currents or a diagenetic effect related to the genesis of nodules.

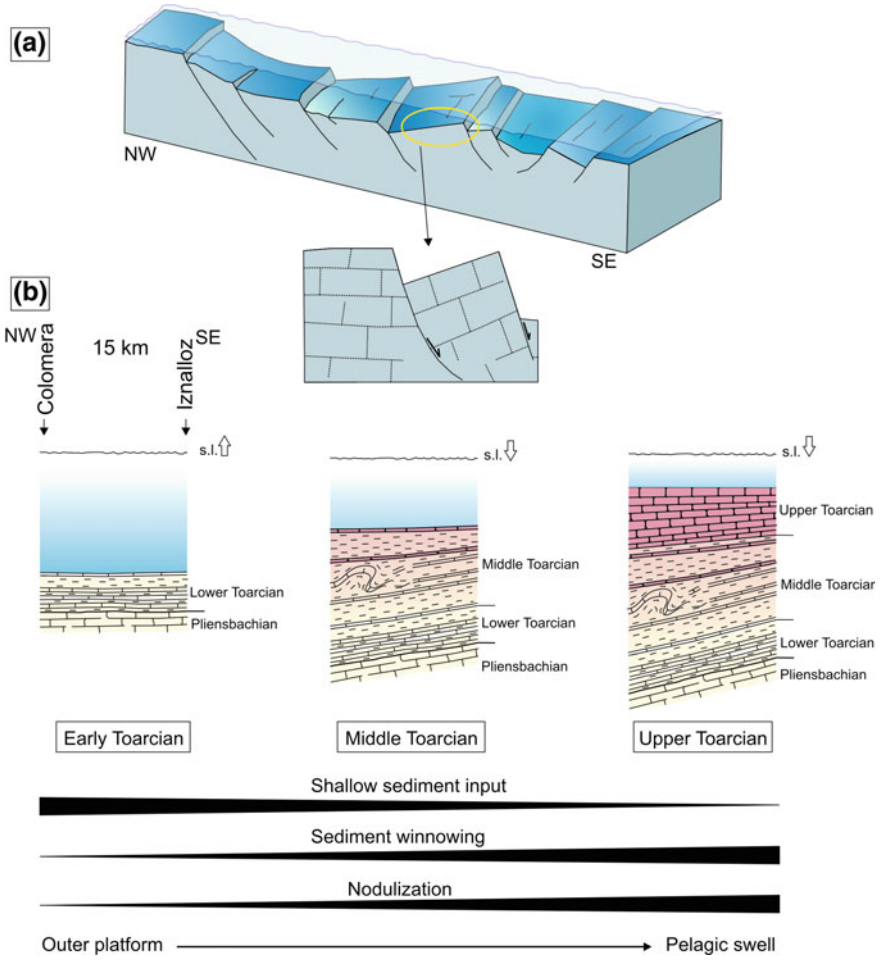

Fig. 4.16 Interpretative model for the Lower Toarcian of the Median Subbetic. **a** Transect of the Median Subbetic. **b** Evolution of the Colomera-Iznalloz transect during the Toarcian with the progressive fragmentation of the carbonate platform and tilting of blocks

Nanno-organisms may have been destroyed by recrystallisation as occurred with overgrown specimens of *Schizosphaerella*, with development of secondary fringes).

Clay minerals (illite, smectite, chlorite and kaolinite) are the main allochthonous component. The white laminated limestones occurring in the Iznalloz section, other allochthonous deposits, are not recorded in the Arroyo Mingarrón and Colomera sections.

The nodular appearance of the ammonitico rosso is mainly related to the combined action of burrowing and compaction. Dissolution appears to be important only at the top of the section (Aalensis Zone), where spheroidal nodules with sharp edges occur.

Previous researches on the nodular formation of ammonitico rosso facies proposed early marine dissolution of mainly aragonitic shells and subsequent reprecipitation as the cause of the lithification and then the formation of nodules. Factors controlling dissolution and cementation, and the early marine nodular lithification, include the submarine winnowing of the carbonate mud at the seafloor and the alteration of sediment properties by burrowing (e.g., Kennedy and Garrison 1975; Mullins et al. 1980).

The original sediment was probably a homogeneous mix of clay minerals, micrite, and bioclasts (calcitic such as crinoids and aragonitic such as ammonoid shells). In a context of low sedimentation rate, e.g., pelagic swells, the dissolution of aragonite produces the Ca^{2+} and HCO_3^- saturation of pore-water in the sediment-water interface and the precipitation of Mg-rich polymorphs of calcite. Therefore, an early diagenetic microenvironmental differentiation (incipient nodulation) of the micritic matrix takes place in the marine porewater zone close to the sediment-sea-water interface. Yet as sedimentation advances, it produces the upward migration of the sediment-water interface, and the input of Ca^{2+} and HCO_3^- into the precipitation horizon (where nodules are growing) is reduced. Finally, a new precipitation horizon begins in the sediment-water interface when saturation is reached. Polished slab with different nodular horizons clearly shows this upward migration process (Fig. 4.9). There is evidence of carbonate-solution processes during the early diagenesis in the ammonitico rosso of the Arroyo Mingarrón and Iznalloz sections, with a selective solution of carbonate in some parts of the sediment and its precipitation in other parts, forming nodules (Reolid et al. 2015). A frequent effect of dissolution is the disappearance of radiolarids in the matrix. Different intensities of the solution-precipitation processes result in variable nodule edge grading from diffuse (Bifrons to Reynesi zones) to sharp (Aalensis Zone). At the top of the Iznalloz and Arroyo Mingarrón sections, in calcareous ammonitico rosso facies from the Aalensis Zone, the growth of the nodules proceeded to the extent of coalescence to produce a semicontinuous or continuous layer of interlocking nodules or a massive rock band. In an extreme case, the reddish matrix is comparatively clay-rich and has a fluidal appearance due to the arrangement of filaments.

Moreover, topographic sea-bottom highs from oceanic and epi-oceanic domains are often affected by increased current intensity because of the interaction of bottom currents with local topography. Enhanced current velocities provide a mechanism for seawater circulation in the uppermost sediment column, thereby providing Ca^{2+} and HCO_3^- for early cementation in the sediment-water interface (McLaughlin and Brett 2004), and triggering early marine lithification (e.g., Mullins et al. 1980; Comas et al. 1981; Reolid et al. 2010). An increased current velocity and hence a decreased sediment accumulation would be expected during sea-level lowstand conditions, such as after the Early Toarcian sea-level maximum (Haq et al. 1987; Hallam 1988, 2001; Jacquin and de Graciansky 1998).

The differentiation between carbonate-rich and clay-rich areas within the sediment, in association with nodulation, is also favoured by burrowing (Fürsich 1973, 1979). Organic (mucilaginous) substances on the walls of some trace fossils, as well as organic matter in the sediment infilling the gallery, could favour dissolution-reprecipitation processes in two opposite ways: (a) it could imply higher alkalinity and selective cementation (Fürsich 1973), or (b) the organic matter might produce acid porewater within the gallery infilling sediment, leading to selective dissolution of early diagenetic carbonate cements and the subsequent heterogeneous compaction of the sediment resulting in nodularity (Eller 1981). Given the abundance of burrows in the nodular limestones of the Iznalloz section, it is evident that the activity of burrowers enhanced sediment permeability and porewater circulation, and thus the dissolution-reprecipitation processes. The composition and abundance of trace fossils from the red nodular limestones (calcareous ammonitico rosso) and nodular marly limestones (marly ammonitico rosso) agree with the influence of bioturbation on nodular appearance, mainly in the Iznalloz section (Reolid et al. 2015).

Finally, synsedimentary rework of sediment with different lithification degrees on the talus slope of epi-oceanic swells could contribute to nodulation, as described by Coudray and Michel (1981), Elmi (1981), and Elmi and Ameur (1984), among others. The presence of slumps and intraclasts would confirm this resedimentation. However, there is no evidence of biogenic encrustations or borings on nodules, so that intense exhumation processes affecting nodules may be excluded.

References

Berner RA (1969) Goethite stability and the origin of red beds. Geochim Cosmochim Acta 33:267–273

Bosellini A (1973) Modello geodinamico e paleotettonico delle Alpi Meridionali durante il Giurassico–Cretacico. Sue possibili applicazioni agli Appennini. In: Accordi B (ed) Moderne vedute sulla Geologia dell'Appennino. Accademia Nazionale Lincei, Quaderni 183:163–205

Boulila S, Galbrum B, Huret E, Hinnov LA, Rouget I, Gardin S, Bartolini A (2014) Astronomical calibration of the Toarcian Stage: implications for sequence stratigraphy and duration of the early Toarcian OAE. Earth Planet Sci Lett 386:98–111

Braga JC, Comas MC, Delgado F, García-Hernández M, Jiménez AP, Linares A, Rivas P, Vera JA (1981) The Liassic Rosso Ammonitico facies in the subbetic zone (Spain). Genetic consideration. In: Farinacci A, Elmi S (eds) Rosso ammonitico symposium proceedings. Tecnocienza, Rome, pp 61–76

Caracuel JE, Monaco P, Olóriz F (1997) Eventos de depósito y colonización del substrato en facies ammonitico rosso (Subbético externo, Kimmeridgiense). Geogaceta 21:63–65

Caracuel JE, Monaco P, Olóriz F (2000) Taphonomic tools to evaluate sedimentation rates and stratigraphic completeness in rosso ammonitico facies (epioceanic tethyan Jurassic). Riv Ital Paleontol Stratigr 106:353–368

Cecca F, Fourcade E, Azéma J (1992) The disappearance of the "Ammonitico Rosso". Palaeogeogr Palaeoclimatol Palaeoecol 99:55–70

Chester R, Baxter GB, Behairy AKA, Connor K, Cross D, Elderfield H, Padgham RC (1977) Soil-sized eolian dusts from the lower troposphere of the eastern Mediterranean Sea. Mar Geol 24:201–217

Comas MC, Olóriz F, Tavera JM (1981) The red nodular limestones (Ammonitico Rosso) and associated facies: a key for settling slopes or swell areas in the Subbetic Upper Jurassic submarine topography (southern Spain). In: Farinacci A, Elmi S (eds) Rosso ammonitico symposium proceedings. Tecnocienza, Rome, pp 113–136

Coudray J, Michel D (1981) Analyse sédimentologique des "calcaires noduleux" qui encadrent les radiolarites du dinantien de la Montagne Noire (France) et apport des donnes expérimentales a la compréhension de leur genèse. In: Farinacci A, Elmi S (eds) Proceedings Rosso Ammonitico Symposium. Tecnoscienza, Rome, pp 149–167

D'Argenio B (1974) Le Piattaforme Carbonatiche Periadriatiche. Una rassegna di problemi nel quadro geodinámico del'area mediterranea. Mem Soc Geol Ital 13:1–28

Dera G, Pellenard P, Neige P, Deconinck JF, Puceat E, Dommergues JL (2009) Distribution of clay minerals in Early Jurassic Peritethyan seas: palaeoclimatic significance inferred from multiproxy comparisons. Palaeogeogr Palaeoclimatol Palaeoecol 271:39–51

Dera G, Brigaud B, Monna F, Laffont R, Puceat E, Deconinck JF, Pellenard P, Joachimski MM, Durlet C (2011) Climatic ups and downs in a disturbed Jurassic world. Geology 39:215–218

Dercourt J, Zonenshain LP, Ricou LE, Kazmin VG, Le Pichon X, Knipper AL, Grandjacquet C, Sborshchikov IM, Boulin J, Sorokhtin O, Geyssant J, Lepvrier C, Biju-Duval B, Sibuet JC, Savostin LA, Westphal M, Lauer JP (1985) Presentation de 9 cartes paléogéographiques a 1:20.000.000 s'étendent de l'Atlantique au Pamir pour la période du Lias à l'actuel. Bull Soc Géol Fr 8:635–652

El Kadiri K (2002) "Tectono-eustatic sequences" of the Jurassic successions from the Dorsale Calcaire (Internal Rif, Morocco): evidence from an eustatic and tectonic scenario. Geol Romana 36:71–103

Eller MG (1981) The red chalk of Eastern England: a Cretaceous analogue of rosso ammonitico. In: Farinacci A, Elmi S (eds) Rosso ammonitico symposium proceedings. Tecnocienza, Rome, pp 207–231

Elmi S (1981) Sédimentation rythmique et organisation séquentielle dans les ammonitico-rosso et les facies associes du Jurassique de la Méditerranée Occidentale. Interpretation des grumeaux et des nodules. In: Farinacci A, Elmi S (eds) Rosso ammonitico symposium proceedings. Tecnocienza, Rome, pp 251–299

Elmi S, Almeras Y (1984) Physiography, palaeotectonics and palaeoenvironments as controls of changes in ammonite and brachiopod communities (an example from the early and middle Jurassic of western Algeria). Palaeogeogr Palaeoclimatol Palaeoecol 47:347–360

Elmi S, Ameur M (1984) Quelques environnements des facies noduleux mésogées. Geol Romana 23:13–22

Ettaki M, Chellaï EH (2005) Le Toarcien inférieur du Haut Atlas de Todrha-Dadès (Maroc): sedimentologie et lithostratigraphie. C R Géosci 337:814–823

Ettaki M, Chellaï EH, Milhi A, Sadki D, Boudchiche L (2000) Le passage Lias moyen-Lias supérieur dans la région de Todrha-Dadès: événements biosédimentaires et géodynamiques (Haut Atlas central, Maroc). C R Acad Sci, Paris 331:667–674

Funk H, Oberhanski R, Pfiffner A, Schmid S, Wildi W (1987) The evolution of the northern margin of Tethys in eastern Switzerland. Episodes 10:102–106

Fürsich FT (1973) *Thalassinoides* and the origin of nodular limestone in the Corallian Beds (Upper Jurassic) of southern England. Neues Jb Geol Paläontol Abh 3:136–156

Fürsich FT (1979) Genesis, environments, and ecology of Jurassic hardgrounds. Neues Jb Geol Paläontol Abh 158:1–163

Gómez JJ, Fernández-López SR (1994) Condensation processes in shallow platforms. Sed Geol 92:147–159

Gong Y (2001) Trace fossils from the flysch sequences of the Silurian, Carboniferous and Triassic of the Tianshan and Kunlun-Qinling orogenic belts of northwestern China. Acta Palaeontol Sin 40:177–188

Gradstein FM, Ogg JG, Smith AG (2004) A geologic time scale 2004. Cambridge University Press
Hallam A (1967) Sedimentology and palaeogeographic significance of certain red limestones and associated beds in the Lias of the Alpine region. Scott J Geol 3:195–220
Hallam A (1988) A reevaluation of Jurassic eustasy in the light of new data and the revised Exxon curve. SEPM Special Publication 42, pp 261–273
Hallam A (2001) A review of the broad pattern of Jurassic sea-level changes and their possible causes in the light of current knowledge. Palaeogeogr Palaeoclimatol Palaeoecol 167:23–37
Han Y, Pickerill RK (1994) *Phycodes templus* isp. nov. from the Lower Devonian of northwestern New Brunswick, eastern Canada. Atlantic Geol 30:37–46
Haq BU, Hardenbol J, Vail PR (1987) Chronology of fluctuating sea level since the Triassic. Science 235:1156–1167
Helm C (2005) Riffe und fazielle Entwicklung der florigemma-Bank (Korallenoolith, Oxfordium) im Süntel und östlichen Wesergebirge (NW-Deustchland). Geol Beitr Hannover 7:1–39
Hermoso M, Pellenard P (2014) Continental weathering and climatic changes inferred from clay mineralogy and paired carbon isotopes across the early to middle Toarcian in the Paris Basin. Palaeogeogr Palaeoclimatol Palaeoecol 399:385–393
Jacquin TH, De Graciansky PC (1998) Major transgressive/regressive cycles: the stratigraphic signature of European basin development. In: De Graciansky PC, Hardenbol J, Jacquin TH, Vail PR (eds) Mesozoic and Cenozoic Sequence Stratigraphy of Europena Basins. SEPM Special Publication 60, pp 15–29
Jenkyns HC (1971) The genesis of condensed sequences in the Tethyan Jurassic. Lethaia 4:327–352
Jiménez AP (1986) Estudio paleontológico de los ammonites del Toarciense inferior y medio de las Cordilleras Béticas (Dactylioceratidae e Hildoceratidae). Ph.D. Thesis, Universidad de Granada
Kennedy WJ, Garrison RE (1975) Morphology and genesis of nodular chalks and hardgrounds in the Upper Cretaceous of southern England. Sedimentology 22:311–386
Krencker FN, Bodin S, Suan G, Heimhofer U, Kabiri L, Immenhauser A (2015) Toarcian extreme warmth led to tropical cyclone intensification. Earth Planet Sci Lett 425:120–130
Mángano MG, Carmona NB, Buatois LA, Muñiz Guinea F (2005) A new ichnospecies of *Arthrophycus* from the Upper Cambrian-Lower Tremadocian of northwest Argentina: implications for the Arthrophycid lineage and potential in ichnostratigraphy. Ichnos 12:179–190
Marok A, Reolid M (2012) Lower Jurassic sediments from the Rhar Roubane Mountains (Western Algeria): Stratigraphic precisions and synsedimentary block-faulting. J Afr Earth Sc 76:50–65
Mattioli E, Erba E (1999) Synthesis of calcareous nannofossil events in tethyan Lower and Middle Jurassic successions. Riv Ital Paleontol Stratigr 105:343–376
Mattioli E, Pittet B, Bucefalo-Palliani R, Röhl HJ, Schmid-Röhl A, Morettini E (2004) Phytoplankton evidence for the timing and correlation of palaeoceanographical changes during the early Toarcian oceanic anoxic event (Early Jurassic). J Geol Soc London 161:685–693
Mattioli E, Plancq J, Boussaha M, Duarte LV, Pittet B (2013) Calcareous nannofossil biostratigraphy: new data from the Lower Jurassic of the Lusitanian Basin. Comunicações Geológicas 100, Especial I:69–76
McLaughlin PI, Brett CE (2004) Sequence stratigraphy and stratinomy of marine hardgrounds: examples from the Middle Paleozoic of Eastern Laurentia. Geological Society of America, Abstracts with programs 36, p 110
Miller W III (2001) *Thalassinoides-Phycodes* compound burrow systems in Paleocene deep-water limestone, Southern Alps of Italy. Palaeogeogr Palaeoclimatol Palaecoecol 170:149–156
Monaco P, Trecci T (2014) Ichnocoenosis in the macigno turbidite basin system, lower miocene, trasimero (Umbrian apennines, Italy). Ital J Geosci 133:116–130
Monaco P, Caracuel JE, Giannetti A, Soria JM, Yébenes A (2007) *Thalassinoides* and *Ophiomorpha* as cross-facies trace fossils of crustaceans from shallow-to-deep-water environments: Mesozoic and Tertiary examples from Italy and Spain. In: 3rd Symposium on Mesozoic and Cenozoic Decapod Crustaceans, Museo di Storia Naturale di Milano, pp 79–82

Mouterde R, Linares A (1960) Nuevo yacimiento fosilífero del Lías superior, cerca de Iznalloz (Provincia de Granada, Cordillera Bética). Notas Comun IGME 58:101–104
Mullins HT, Neumann AC, Wilber RJ, Boardman MR (1980) Nodular carbonate sediment on Bahamian slopes: possible precursor to nodular limestones. J Sediment Petrol 50:117–131
Nieto LM, Ruiz-Ortiz PA Rey J, Benito MI (2008) Strontium-isotope stratigraphy as a constraint on the age of condensed levels: examples from the Jurassic of the Subbetic Zone (southern Spain). Sedimentology 55:1–29
Nieto LM, Rodríguez-Tovar FJ, Molina JM, Reolid M, Ruiz-Ortiz PA (2014) Unconformity surfaces in pelagic carbonate environments: a case from the Middle Bathonian of the Betic Cordillera, SE Spain. Ann Soc Geol Pol 84:281–295
Ogg J, Hinnov LA (2012) The Jurassic period. In: Gradstein F, Ogg J, Ogg G, Smith D (eds) A geologic time scale 2012. Elsevier, pp 731–791
Oliveira LCV, Perilli N, Duarte LV (2007) Calcareous nannofossil assemblages around the Pliensbachian/Toarcian boundary in the reference section of Peniche (Portugal). Ciências Terra (UNL) 16:45–50
Olóriz F, Reolid M, Rodríguez-Tovar FJ (2012) Palaeogeography and relative sea-level history forcing eco-sedimentary contexts in Late Jurassic epicontinental shelves (Prebetic Zone, Betic Cordillera): an ecostratigraphic approach. Earth Sci Rev 111:154–178
Palomo I (1987) Mineralogía y geoquímica de sedimentos pelágicos del Jurásico inferior de las Cordilleras Béticas (SE de España). Ph.D. Thesis, Universidad de Granada
Parisi G, Ortega-Huertas M, Nocchi M, Palomo I, Monaco P, Ruiz F (1996) Stratigraphy and geochemical anomalies of the Early Toarcian oxygen-poor interval in the Umbria-Marche Apennines (Italy). Geobios 29:469–484
Petrash DA, Lalonde SV, Gingras MK, Konhauser KO (2010) A surrogate approach to studying the chemical reactivity of burrow mucous lining in marine sediments. Palaios 26:594–600
Reolid M (2014) Stable isotopes on foraminifera and ostracods for interpreting incidence of the Toarcian Oceanic Anoxic Event in Westernmost Tethys: role of water stagnation and productivity. Palaeogeogr Palaeoclimatol Palaeoecol 395:77–91
Reolid M, Nagy J, Rodríguez-Tovar FJ, Olóriz F (2008) Foraminiferal assemblages as palaeoenvironmental bioindicators in Late Jurassic epicontinental platforms: relation with trophic conditions. Acta Palaeontol Pol 53:706–722
Reolid M, Molina JM, Löser H, Navarro V, Ruiz-Ortiz PA (2009) Coral biostromes of the Middle Jurassic from the Subbetic (Betic Cordillera, southern Spain): facies, coral taxonomy, taphonomy and palaeoecology. Facies 55:575–593
Reolid M, Nieto LM, Rey J (2010) Taphonomy of cephalopod assemblages from Middle Jurassic hardgrounds of pelagic swells (South-Iberian palaeomargin, Western Tethys). Palaeogeogr Palaeoclimatol Palaeoecol 292:257–271
Reolid M, Sebane A, Rodríguez-Tovar FJ, Marok A (2012a) Foraminiferal morphogroups as a tool to approach the Toarcian Anoxic Event in the Western Saharan Atlas (Algeria). Palaeogeogr Palaeoclimatol Palaeoecol 323–325:87–99
Reolid M, Rodríguez-Tovar FJ, Marok A, Sebane A (2012b) The Toarcian Oceanic Anoxic Event in the Western Saharan Atlas, Algeria (North African paleomargin): role of anoxia and productivity. Geol Soc Am Bull 124:1646–1664
Reolid M, Chakiri S, Bejjaji Z (2013a) Adaptative strategies of the Toarcian benthic foraminiferal assemblages from the Middle Atlas (Morocco): palaeoecological implications. J Afr Earth Sc 84:1–12
Reolid M, Nieto LM, Sánchez-Almazo IM (2013b) Caracterización geoquímica de facies pobremente oxigenadas en el Toarciense inferior (Jurásico inferior) del Subbético Externo. Rev Soc Geol Esp 26:69–84
Reolid M, Marok A, Sebane A (2014a) Foraminiferal assemblages and geochemistry for interpreting the incidence of Early Toarcian environmental changes in North Gondwana palaeomargin (Traras Mountains, Algeria). J Afr Earth Sc 95:105–122

Reolid M, Mattioli E, Nieto LM, Rodríguez-Tovar FJ (2014b) The Early Toarcian Ocanic Anoxic Event in the External Subbetic (Southiberian Palaeomargin, Westernmost Tethys): geochemistry, nannofossils and ichnology. Palaeogeogr Palaeoclimatol Palaeoecol 411:79–94

Reolid M, Rivas P, Rodríguez-Tovar FJ (2015) Toarcian ammonitico rosso facies from the South Iberian paleomargin (Betic Cordillera, southern Spain): paleoenvironmental reconstruction. Facies 61:22. doi:10.1007/s10347-015-0447-3

Rita P, Reolid M, Duarte LV (2016) Benthic foraminiferal assemblages record major environmental perturbations during the Late Pliensbachian—Early Toarcian interval in the Peniche GSSP, Portugal. Palaeogeogr Palaeoclimatol Palaeoecol 454:267–281

Rivas P (1972) Estudio paleontológico-estratigráfico del Lías (Sector Central de las Cordilleras Béticas). Ph.D. Thesis, Universidad de Granada, Short Publication 29, p 77

Rodríguez-Tovar FJ, Nieto LM (2013) Composite trace fossil assemblage in a distal carbonate setting from the Tethys (Middle Jurassic, Betic Cordillera, Southern Spain). Ichnos 20:43–53

Rodríguez-Tovar FJ, Reolid M (2013) Environmental conditions during the Toarcian Oceanic Anoxic Event (T-OAE) in the westernmost Tethys: influence of the regional context on a global phenomenon. Bull Geosci 88:697–712

Rodríguez-Tovar FJ, Uchman A (2010) Ichnofabric evidence for the lack of bottom anoxia during the lower Toarcian Oceanic Anoxic Event (T-OAE) in the Fuente de la Vidriera section, Betic Cordillera, Spain. Palaios 25:576–587

Rozic B, Smuc A (2011) Gravity-flow deposits in the Toarcian Perbla formation (Slovenian basin, NW Slovenia). Riv Ital Paleontol Stratigr 117:283–294

Ruebsam W, Münzberger P, Schwark L (2014) Chronology of the Early Toarcian environmental crisis in the Lorraine Sub-basin (NE Paris Basin). Earth Planet Sci Lett 404:273–282

Sandoval J, Bill M, Aguado R, O'Dogherty L, Rivas P, Morard A, Guex J (2012) The Toarcian in the Subbetic basin (southern Spain): bio-events (ammonite and calcareous nannofossils) and carbon-isotope stratigraphy. Palaeogeogr Palaeoclimatol Palaeoecol 342–343:40–63

Santantonio M (1993) Facies associations and evolution of pelagic carbonate platform/basin systems: examples from the Italian Jurassic. Sedimentology 40:1039–1067

Santantonio M (1994) Pelagic carbonate platforms in the geologic record: their classification, and sedimentary and paleotectonic evolution. AAPG Bull 78:122–141

Savrda CE (2012) Chalk and related deep-marine carbonates. In: Knaust D, Bromley RG (eds) Trace fossils as indicators of sedimentary environments. Development in Sedimentology 64, pp 777–806

Soussi M, Ben Ismail MH (2000) Platform collapse and pelagic seamount facies: Jurassic development of central Tunisia. Sed Geol 133:93–113

Soussi M, Enay R, Mangold C, Turki MM (2000) The Jurassic events and their sedimentary and stratigraphic records on the Southern Tethyan margin in Central Tunisia. Mém Mus Natl d'Hist Nat, Paris 182:57–92

Uchman A, Tchoumatchenco P (2003) A mixed assemblage of deep-sea and shelf trace fossils from the Lower Cretaceous (Valanginian) Kamchia Formation in the Troyan Region, Central Fore-Balkan, Bulgaria. Ann Soc Geol Pol 73:27–34

Vera JA (1988) Evolución de los sistemas de depósito en el Margen Ibérico de la Cordillera Bética. Rev Soc Geol Esp 1:373–391

Vogel K, Bundschuh M, Glaub I, Hofmann K, Radtke G, Schmidt H (1995) Hard substrate ichnocoenoses and their relations to light intensity and marine bathymetry. Neues Jb Geol Paläontol Abh 195:49–61

Winterer EL, Bosellini A (1981) Subsidence and sedimentation on Jurassic passive continental margin, Southern Alps, Italy. AAPG Bull 65:394–421

Yelles-Chaouche AK, Ait-Ouali R, Bracène R, Derder MEM, Djellit H (2001) Chronologie de l'ouverture du bassin des Ksour (Atlas Saharien, Algérie) au début du Mésozoïque. Bull Soc Géol Fr 172:285–293